

SLAC - PUB - 3725
June 1985
(T/E)

RADIATIVE CORRECTIONS IN $SU_2 \times U_1$:
LEP/SLC

B. W. LYNN* AND M. E. PESKIN*

*Stanford Linear Accelerator Center
Stanford University, Stanford, California, 94305*

and

R. G. STUART

CERN, CH-1211 Geneva 23, Switzerland

ABSTRACT

We show the sensitivity of various experimental measurements to one-loop radiative corrections in $SU_2 \times U_1$. Models considered are the standard GSW model as well as extensions of it which include extra quarks and leptons, SUSY and certain technicolor models. The observation of longitudinal polarization is a great help in seeing these effects in asymmetries in $e^+e^- \rightarrow \mu^+\mu^-, \tau^+\tau^-$ on Z^0 resonance.

Contribution to LEP Physics Study Group, "Precision Tests of the Standard Model at the Z^0 ", Geneva, Switzerland, March 19, 1985.

To appear in Proceedings of LEP Physics Workshop
(LEP "yellow book"), CERN Report 1985.

* Work supported by the Department of Energy, contract DE - AC03 - 76SF00515.

1. Introduction

One of the central questions of high-energy physics is that of determining what theory underlies the standard weak-interaction model of Glashow, Salam, and Weinberg (GSW) at distances much shorter than those we currently explore. The standard model has had dramatic success in predicting the features of the weak neutral current and in locating the masses of the W and Z bosons. But it is a theory which leaves undetermined a very large number of fundamental parameters, including a dimensionful parameter, the mass of the Higgs boson. If these parameters are truly determined by theory and not just put in *ad hoc*, then we must find a still more fundamental theory which reduces to the standard model at ordinary energies. Where do we look for signs that the standard model requires correction in this way? In many specific schemes which have been explored, the first sign of the presence of a new level of physics beyond the standard model is the appearance of novel particles associated with excitations in the new sector. Because of this, the search for novel particles has been a major preoccupation of physicists working at the highest-energy e^+e^- and $p\bar{p}$ colliders. In the late 1980's, SLC, LEP, and the HERA and Tevatron colliders will explore for new states in the mass region up to about 100 GeV.¹ Further direct exploration will need to wait for the large hadron-hadron colliders planned for the 1990's.

One might well hope to evade the requirement of attaining increasingly higher center-of-mass energies by searching for indirect effects of the new sector. The most sensitive such searches, however, have required that the new states make themselves visible through couplings which change quark or lepton flavor. Such indirect searches have had far less power when the new states couple to ordinary matter in a way that does not depend on flavor, as, for example, if they couple

to ordinary matter only via the weak gauge bosons.

This situation will change, however, when the Z^0 resonance is produced in e^+e^- collisions at SLC and LEP, and when W bosons are produced in quantity at the Tevatron and at LEP2. The W and Z couple directly to all particles, familiar or novel, which have weak interactions. Even those particles which are too heavy to be pair-produced at the Z^0 will affect the properties of these resonances through their virtual effects in loop diagrams. These loop effects are, in general, quite small, correcting the mass of the Z^0 by amounts of relative size $\alpha/\pi \sim 10^{-3}$. But the Z and W are elementary, weakly-interacting objects whose properties can be computed precisely by Feynman diagrams; they are also prominent resonances, with certain specific properties which allow precision experiments. We judge that the available technology, both experimental and theoretical, is sufficient that such tiny effects can be unambiguously observed.¹

There is one conceptual problem in isolating these loop effects which we should now discuss. Since these effects are typically of order 0.1% in size, their identification requires determining the parameters of the standard model to an accuracy of 0.1% or better. The standard model contains three parameters to which the properties of the Z^0 are directly sensitive: the two gauge coupling constants g and g' and the Higgs vacuum expectation value v (or, alternatively, the fine structure constant α , the W mass, and the Z^0 mass). These are of special importance because they enter the tree-level expressions for leptonic processes. To define these parameters, we will recast them as the combinations:

$$\alpha, M_Z, \text{ and } G_\mu. \tag{1.1}$$

M_Z is conventionally defined as the position of the pole in the Z propagator; this

mass can be straightforwardly extracted from the shape of the Z^0 resonance. α is given by the electron charge from Thomson scattering measured at $q^2 = 0$. G_μ is conventionally defined from the muon lifetime τ_μ by extracting specific purely electromagnetic radiative corrections:

$$\begin{aligned} \tau_\mu^{-1} = & \frac{G_\mu^2 m_\mu^5}{192\pi^3} \left[1 + \frac{\alpha}{2\pi} \left(\frac{25}{4} - \pi^2 \right) \left(1 + \frac{2\alpha}{3\pi} \ln \frac{m_\mu}{m_e} \right) \right] \\ & \times \left[1 + \frac{3}{5} \frac{m_\mu^2}{M_W^2} \right] \left[1 - 8 \frac{m_e^2}{m_\mu^2} \right]. \end{aligned} \quad (1.2)$$

A recent CERN experiment by G. Bardin *et. al.*² gives

$$G_\mu = (1.16637 \pm 0.00002) \times 10^{-5} \text{ GeV}^{-2}. \quad (1.3)$$

G_μ and α are the best known electroweak constants of Nature. LEP and SLC will soon measure M_Z to 4 significant figures, an accuracy adequate for our purposes.

To completely specify the GSW model, one must also provide values for the Higgs boson self-coupling λ (or, alternatively, the Higgs boson mass m_H), the fermion masses m_f , and the quark mixing angles θ_i . The expressions we will eventually derive will depend weakly on m_H and on m_t , the top quark mass. For these parameters, we will simply choose standard values—100 GeV for m_H and 30 GeV for m_t —and use these, except where we state otherwise, in all of our calculations. We will, of course, display separately the dependence of our results on m_H and m_t .

To test the standard model, and to find new contributions which go beyond it, one needs an additional experiment which can provide the same level of accuracy.

One such experiment, which is difficult but conceptually quite familiar, is the accurate determination of the W boson mass. In this paper, we would like to emphasize a second set of experiments at LEP/SLC; the various asymmetries in $e^+e^- \rightarrow \mu^+\mu^-, \tau^+\tau^-$. We will show that these asymmetries, measured on Z^0 resonance where statistics are expected to be good, will test the GSW model at the one-loop level and possibly reveal the existence of particles beyond GSW. We will further show that the ability to observe longitudinal polarization, either in initial-state electron beams or in final state τ^- polarization, is especially useful for probing radiative corrections.

An auxiliary quantity which will enter our analysis is $\sin^2 \theta_w$. It is not a free parameter but rather only a bookkeeping device to be defined in terms of the set (1.1) and m_H, m_t . Sirlin has introduced the convention of defining $\sin^2 \theta_w$ in terms of the measured W and Z boson masses.³ This definition is a very sensible one for $SU(2) \times U(1)$ (but less clear for other gauge groups) because it is in principle unambiguous. It is also a very convenient definition for the following reason: One part of the 1-loop correction to any weak process for $q^2 \sim -M_Z^2$ arises from the renormalization of α from $q^2 = 0$ to $q^2 = -M_Z^2$ due to QED vacuum polarization diagrams like those in Fig. 1. This correction is universal (g and g' are renormalized the same way by the large logs from photon vacuum polarization fermion loops) and is present in any theory which unifies weak and electromagnetic interactions. Marciano⁴ has pointed out this correction makes an unusually large contribution to the W boson mass. It is also the largest correction to the lepton pair production polarization asymmetry.⁵ (Observation of the shift in the longitudinal polarization asymmetry or some other weak process due these QED corrections would indicate that $\alpha_2 = g^2/4\pi$ is renormalized the

same way by the large logs from the diagrams in Fig. 1 as is α and that therefore some sort of unification of weak and electromagnetic interactions is correct.) Including the QED renormalization effect in the definition of $\sin^2 \theta_w$, then, greatly reduces the size of all standard model weak radiative corrections. We would prefer, however, to define $\sin^2 \theta_w$ so that it can be determined simply from the measurement of α , G_μ , and M_Z . We therefore chose to define θ_w by the formula:⁶

$$\sin 2\theta_w \equiv \left(\frac{4\pi\alpha}{\sqrt{2}G_\mu M_Z^2 \cdot (1 - \Delta r_0)} \right)^{1/2}, \quad (1.4)$$

where

$$\Delta r_0 \equiv 0.06. \quad (1.5)$$

This factor corrects the zeroth-order Born formulae to include the effect of the renormalization of α ; our precise choice is made to establish a convention. A more precise evaluation of the QED renormalization factor^{3,7,8} for $q^2 \gg m_f^2$ reduces to

$$\Delta r_{\text{QED}}^{\text{free fields}} = \frac{\alpha}{3\pi} \sum_{\text{fermions}} Q_f^2 \mathcal{N}_c \left(\ln \frac{-q^2}{m_f^2} - \frac{5}{3} \right) \quad (1.6)$$

for light quarks and leptons when strong interactions are neglected. Here $\mathcal{N}_c = 3(1)$ is the number of colors for quarks(leptons) and Q_f is the fermion electric charge; $Q_e = -1$ for electrons. To compute Δr_{QED} properly, one includes the effects of strong interactions; hadronization of the light quarks, u, d, c, s is taken into account via a dispersion relation in $e^+e^- \rightarrow \text{hadrons}$ while the t and b quarks and e, μ and τ are treated as free particles. An accurate evaluation of this

correction, for $q^2 = -(94 \text{ GeV})^2$, and $m_T = 30 \text{ GeV}$, gives⁷

$$\Delta r_{\text{QED}} = 0.0597 \pm 0.0013 . \quad (1.7)$$

We have displayed an uncertainty due to strong interaction effects and note that it makes its way into one loop radiative corrections even in purely leptonic processes via the renormalization of α . Marciano and Sirlin⁸ have shown that placing the factor $(1 - \Delta r_{\text{QED}})$ in analogy with putting $(1 - \Delta r_0)$ in the denominator of (1.4) sums all of the leading QED infrared logarithms. This definition of $\sin^2 \theta_w$ agrees with that of Sirlin at tree level but differs by $\mathcal{O}(\alpha)$ corrections.

We should warn the reader that the analysis presented here ignores QED radiative corrections associated with radiation of real or virtual photons from external legs, since these corrections depend on details of the particular experimental arrangement. They have been adequately considered by others.⁹ Thus, the graphs of Fig. 2 and all permutations are specifically excluded from our analysis of all four-lepton processes in either t or s channels. We do, however, include the QED vacuum polarization graphs of Fig. 1, as we have discussed.

Our analysis will proceed as follows. In Section 2 we will outline a formalism for the calculation of all one-loop radiative correction effects in four-lepton processes and will derive there effective matrix elements for charged and neutral current processes which include all one-loop corrections in $SU_2 \times U_1$ broken primarily by Higgs doublets.⁶ It will be convenient then to divide one-loop corrections into two groups: *oblique corrections* affecting only gauge-boson vacuum polarization amplitudes and *direct corrections* involving 1PI vertex, fermion self-energy and box corrections. The first class, oblique, includes all of those corrections which do not involve the external particles. Examples are vector-ghost graphs,

extra quarks and leptons, squarks, technicolor, and small effects due to v.e.v.'s of scalars transforming in SU_2 representations different from doublets. The second class include all those corrections involving the external particles; examples are many supersymmetric particles—winos, neutralinos, the first two generations of sleptons—and some extended technicolor models which are expected to give masses to the light leptons. For oblique couplings all one-loop radiative corrections can be absorbed into four functions; this is a great help in classifying the effects of new particles. In Section 3 we will define some physical quantities: the initial state longitudinal polarization, forward-backward, transverse polarization and final-state τ^- polarization asymmetries in $e^+e^- \rightarrow \mu^+\mu^-, \tau^+\tau^-$, the ratio of Bhabha scattering to μ pair production and the Z^0 width (all measurable at LEP1/SLC) the W^\pm mass and width (measurable at LEP2 and the Tevatron) and various ratios of neutrino scattering on electrons at low q^2 (to be measured by the CHARM II collaboration¹⁰). We give the one-loop GSW prediction for these quantities and show the sensitivity to high Higgs' and top-quark masses. In Section 4, we give the response of the various asymmetries in $e^+e^- \rightarrow \mu^+\mu^-$ and $\tau^+\tau^-$, Bhabha scattering and W^\pm mass to one-loop effects due to new physics; notably extra generations of quarks and leptons, SUSY and Technicolor. In Section 5 we give some conclusions.

Throughout this paper we will use the Euclidean metric, so that on Z^0 resonance $q^2 = \bar{q}^2 - q_0^2 = -M_Z^2$. All work on one-loop radiative corrections in the standard GSW model is from the work of Lynn and Stuart.^{5,11} All work on the contributions to radiative corrections from beyond the standard model is from the work of Lynn¹⁵ and Lynn and Peskin.⁶ We apologize for any references omitted.

2. General Scheme for $SU_2 \times U_1$ Radiative Corrections⁶

To study weak radiative corrections as a function of the kinematic variables associated with a given reaction, it is useful to construct an effective 4-fermion vertex for neutral current processes which includes all of the possible 1-loop subgraphs. We will approach this object in stages. Let us first note that, if the external particles in a process are e , μ , and τ , then at Z^0 energies we may ignore the masses of these particles. That in turn implies that helicity is conserved at each gauge boson vertex. Thus, if we define the polarization of one initial- and one final-state fermion, the process contains only one invariant amplitude. For example, the cross-section for the reaction $e^+e^- \rightarrow \mu^+\mu^-$ takes the form:

$$\frac{d\sigma}{dt} (e^-(P)e^+ \rightarrow \mu^-(P')\mu^+) = \frac{4\pi\alpha^2}{s} \cdot k_{PP'}^2 \cdot |\mathcal{M}_{PP'}(-s)|^2, \quad (2.1)$$

where P and P' denote longitudinal polarizations L or R . $k_{PP'}^2$ is a kinematic factor from the Dirac algebra, equal to $(u/s)^2$ for $L \rightarrow L$ and $R \rightarrow R$ and to $(t/s)^2$ for $L \rightarrow R$ and vice versa. $\mathcal{M}_{PP'}$ is the invariant amplitude which contains all the nontrivial information about the coupling; it is defined in such a way that $\mathcal{M}_{PP'}$ equals 1, independently of P and P' , for the simple s-channel photon exchange diagram of lowest-order QED for electrons. In the GSW theory, at leading order, but generalizing to arbitrary fermions in the initial and final states, \mathcal{M} is given by:

$$\begin{aligned}
M_{PP'}(q^2) &= Q \frac{-s}{q^2} Q' \\
&+ \left(\frac{I^3 - Q \sin^2 \theta_w}{\cos \theta_w \sin \theta_w} \right) \frac{-s}{q^2 + M_Z^2 - i \text{Im} \Pi_{ZZ}^{1\text{-loop}}(q^2)} \\
&\times \left(\frac{I^{3'} - Q' \sin^2 \theta_w}{\cos \theta_w \sin \theta_w} \right)
\end{aligned} \tag{2.2}$$

where we have inserted the tree level Z^0 width (imaginary part of the one-loop Z^0 self energy) so that this expression remains finite on resonance. In the case in which only light quarks and leptons can be produced at $s = M_Z^2$ we have¹²

$$\begin{aligned}
\text{Im} \Pi_{ZZ}^{1\text{-loop}}(-M_Z^2) &\equiv \Gamma_Z^0 M_Z \\
&= \frac{\alpha M_Z^2}{3 \sin^2 \theta_w \cos^2 \theta_w} \sum_{\text{fermions}} \left[\left(\frac{I_L^3}{2} - Q \sin^2 \theta_w \right)^2 \left(1 + 2 \frac{m_f^2}{M_Z^2} \right) \right. \\
&\quad \left. + \left(\frac{I_L^3}{2} \right)^2 \left(1 - 4 \frac{m_f^2}{M_Z^2} \right) \right] \cdot \left(1 - 4 \frac{m_f^2}{M_Z^2} \right)^{\frac{1}{2}} \cdot C_{\text{QCD}} .
\end{aligned} \tag{2.3}$$

with fermion masses $2m_f < M_Z$ and left-handed isospin component I_L^3 . The last factor gives the QCD corrections to the lowest order width; C_{QCD} is $3 \cdot (1 + \alpha_{\text{strong}}(-M_Z^2)/\pi)$ for quarks and 1 for leptons.

It is straightforward to add to the above expression for M the effects for all possible 1-loop subdiagrams. At the same time, one must correct the factors of α and G_μ and M_Z in the tree level expression from their bare to their physical values. For simplicity, let us first carry out the analysis only for *oblique* corrections. *Oblique corrections are all of those corrections which affect only vector particle vacuum polarization amplitudes.* These explicitly include the standard

QED corrections of Fig. 1. A typical 1PI vector self energy, a formally infinite object containing no counterterms, is defined in Fig. 3. The calculation of Π_{ij} , $i, j = Z^0, W^\pm, A$ (photon) or $i, j = SU_2$ currents 1, 2, 3 and electromagnetic current Q is clearly just a matter of counting the representations of $SU_2 \times U_1$ particles in the theory and being careful about mass diagonalization and Clebsch-Gordon coefficients.

Including only these oblique corrections, \mathcal{M} takes the form (with the abbreviation $\sin^2 \theta_w = s_\theta^2$)

$$\begin{aligned}
\mathcal{M} = & Q \frac{1}{1 - \Delta_\alpha(q^2)} \left(\frac{-s}{q^2} \right)^2 Q' + \frac{I_3 - Q(s_\theta^2 + \Delta_p(q^2) - is_\theta c_\theta \text{Im} \Pi'_{ZA}(q^2))}{s_\theta c_\theta} \\
& \times \frac{-s}{(q^2 + M_Z^2)(1 - \Delta_\rho(q^2) - 0.06) - \text{Im} \Pi_{ZZ}^{1 \text{ loop}}(q^2)(1 - C_\Gamma \Delta_p(q^2))} \\
& \times \frac{I_3' - Q'(s_\theta^2 + \Delta_p(q^2) - is_\theta c_\theta \text{Im} \Pi'_{ZA}(q^2))}{s_\theta c_\theta}
\end{aligned} \tag{2.4}$$

where

$$\begin{aligned}
\Delta_p(q^2) = & \Delta_p(-M_Z^2) \\
& - 4\pi\alpha \text{Re} \left(\frac{\Pi_{33}(-M_Z^2) - \sin^2 \theta_w \Pi_{3Q}(-M_Z^2)}{M_Z^2} + \frac{\Pi_{33}(q^2) - \sin^2 \theta_w \Pi_{3Q}(q^2)}{q^2} \right)
\end{aligned} \tag{2.5}$$

$$\begin{aligned}
\Delta_\rho(q^2) = & \Delta_\rho(0) \\
& + \text{Re} \left(\frac{\Pi_{ZZ}(-M_Z^2) - \Pi_{ZZ}(0)}{M_Z^2} + \frac{\Pi_{ZZ}(q^2) - \Pi_{ZZ}(-M_Z^2)}{q^2 + M_Z^2} \right)
\end{aligned} \tag{2.6}$$

$$\Delta_\alpha(q^2) = \frac{4\pi\alpha}{q^2} \left(\Pi_{QQ}(q^2) - q^2 \Pi'_{QQ}(0) \right) \tag{2.7}$$

and $\Delta_\rho(0)$, $\Delta_\rho(-M_Z^2)$ are given by

$$\Delta_\rho(0) = \frac{4\pi\alpha}{M_Z^2 \cos^2 \theta_w \sin^2 \theta_w} (\Pi_{33}(0) - \Pi_{11}(0)) \quad (2.8)$$

$$\begin{aligned} \Delta_\rho(-M_Z^2) = & \frac{\sin^2 \theta_w \cos^2 \theta_w}{\cos 2\theta_w} \cdot \text{Re} \left(\Delta_\alpha(-M_Z^2) - \Delta_\rho(0) - 0.06 \right. \\ & \left. - \frac{4\pi\alpha}{\sin^2 \theta_w \cos^2 \theta_w} \frac{1}{M_Z^2} (\Pi_{33}(-M_Z^2) - \Pi_{33}(0) - \Pi_{3Q}(-M_Z^2)) \right). \end{aligned} \quad (2.9)$$

This expression makes obvious the constraint on \mathcal{M} which follows from the renormalizability of the electroweak interactions; it must be free of one-loop divergences. One can see that the various vacuum polarization amplitudes in (2.4) are assembled into combinations whose divergences cancel explicitly. We have replaced the vacuum polarization amplitudes of vector bosons W , Z and A (photon) with vacuum polarization amplitudes of the weak isospin and electromagnetic currents. Denoting the weak isospin currents by 1, 2, 3 and the electromagnetic current by Q , we have

$$\Pi_{AA} = e^2 \Pi_{QQ}, \quad \Pi_{ZA} = \frac{e^2}{\cos \theta_w \sin \theta_w} (\Pi_{3Q} - \sin^2 \theta_w \Pi_{QQ}), \quad (2.10)$$

$$\Pi_{WW} = \frac{e^2}{\sin^2 \theta_w} \Pi_{11}, \quad \Pi_{ZZ} = \frac{e^2}{\sin^2 \theta_w \cos^2 \theta_w} (\Pi_{33} - 2 \sin^2 \theta_w \Pi_{3Q} + \sin^4 \theta_w \Pi_{QQ}).$$

The combination $\Delta_\alpha(q^2)$ is simply the properly subtracted photon vacuum polarization. The combination $\Delta_\rho(q^2)$ is also independently observable, giving at $q^2 = 0$ the one-loop oblique particle correction to the ρ parameter¹³ which mea-

sures the relative strength of charged and neutral weak currents:

$$\rho - 1 = \Delta_\rho(0) . \quad (2.11)$$

The quantity $\Delta_\rho(q^2)$ is also free of ultraviolet divergences: Π_{3Q} vanishes at $q^2 = 0$. It may have a divergent slope at that point, but the relation $Q = I^3 + \frac{Y}{2}$ implies that Π_{33} has an identical (and, thus, cancelling) divergence.

It is easy to see that only three independent combinations of vacuum polarization amplitudes can appear in the most general neutral current matrix element for oblique corrections due to any representations of $SU_2 \times U_1$; there are only three neutral vector self energies: $Z - Z$, $Z - A$ and $A - A$. The fourth possible vector self energy, the $W - W$, will result in a fourth (and last) independent combination which will of course enter into the effective matrix element governing charged-current processes at the one loop-level. It is also easy to see why these particular combinations arise: since we have used α , G_μ and M_Z as renormalized input data, the shift in these quantities from their bare to renormalized values

$$\frac{\delta_b \alpha}{\alpha} = -\Pi'_{AA}(q^2 = 0) \quad (2.12)$$

$$\frac{\delta_b G_\mu}{G_\mu} = -\frac{\Pi_{WW}(q^2 = 0)}{M_W^2} \quad (2.13)$$

$$\frac{\delta_b M_Z^2}{M_Z^2} = \text{Re} \frac{\Pi_{ZZ}(q^2 = -M_Z^2)}{M_Z^2} \quad (2.14)$$

will enter our expressions. Also, the quantities $\Pi_{AA}(q^2)$, $\Pi_{ZZ}(q^2)$ and $\Pi_{ZA}(q^2)$ enter neutral current processes directly. There are also factors of $\Pi_{ZA}(0)$ (when this does not automatically vanish) coming from the Ward identity governing the

SU_2 vector boson wavefunction renormalization but we will drop these throughout this paper. Note the inclusion in (2.4) of the appropriate $O(\alpha^2)$ contributions to the imaginary part of the Z^0 inverse propagator. This is necessary in order that we may examine the corrections to *cross sections* to the 0.1 percent level on the Z^0 resonance; it is not necessary off resonance or for the discussion of *asymmetries* because it cancels out in ratios of cross sections at this level of accuracy. We will discuss the constant C_Γ and why $\Delta_p(q^2)$ alone occurs in the shift in the imaginary part of the Z^0 inverse propagator later.

Equation (2.4) is the main result of this section. It makes explicit (at least for the case of oblique corrections) the reduction of the variety of weak radiative corrections to a few (for oblique corrections there are four) basic quantities which determine the experimentally accessible parameters. In particular, it should be noted that for $e^+e^- \rightarrow f\bar{f}$ with $f \neq e, \nu_e$ on the Z^0 resonance where only the Z propagator term is important, all of the various possible asymmetries and cross sections in fermion pair production are determined entirely by the relative coefficients of I^3 and Q in the fermion-fermion- Z^0 vertex. Thus, all of the asymmetries in $e^+e^- \rightarrow \mu^+\mu^-$ measure the same quantity, $\Delta_p(-M_Z^2)$ and corrections to, say, the charge asymmetry are proportional to those of the polarization asymmetry with the constant of proportionality a function only of $\sin^2 \theta_w$.

We now turn to the direct coupling corrections: 1PI vertex, fermion self energy parts and box diagrams. The box diagrams form a gauge invariant set and so are finite to one-loop. Combinations of 1PI vertex parts and external fermion line self-energies are also finite as we will explain now.

The Ward identities of $SU_2 \times U_1$ govern the relationship between the vector

boson wavefunction renormalizations Z_W (for weak isospin) and Z_B (weak hypercharge) and their respective bare couplings $g^0, g^{0'}$ and the renormalized finite couplings g, g' . In analogy with QED we have ($\sin \theta_w \equiv s_\theta$)

$$Z_B^{1/2} g^{0'} = g' \quad (2.15)$$

$$Z_W^{1/2} g^0 = g \left(1 + \frac{\Pi_{ZA}(0)}{c_\theta s_\theta M_Z^2} \right) + \mathcal{O}(g^5). \quad (2.16)$$

Since exactly the combination $Z_B^{1/2} g^{0'}$ and $Z_W^{1/2} g^0$ occur in the bare Lagrangian, the fermion wavefunction renormalization must also properly subtract the fermion-vector boson vertices. Note that we will drop all factors of $\Pi_{ZA}(0)/c_\theta s_\theta M_Z^2$ which is a non-zero constant for internal gauge boson lines. Consequently, if we divide the 1PI fermion self-energy and fermion-boson vertex parts into left-handed and right-handed parts as in Figs. 4 and 5 with $\gamma_\pm = \frac{1}{2}(1 \pm \gamma_5)$ the left- and right-handed spin projection operators, the combinations

$$\Gamma_\pm^{eez} = \tilde{\Gamma}_\pm^{eez} + \left[A_\pm^e + 2m_e^2 \frac{\partial}{\partial p^2} (C^e - A_\pm^e) \right]_{p^2=-m_e^2} \quad (2.17)$$

will be finite. All other fermion-vector boson couplings are treated in a completely analogous way.

We close this section with a discussion of the effective matrix element to one loop for charged current scattering and its relation to the shift in the W mass. At tree level the W couples only left-handedly and it is easy to see that, neglecting the masses of external particles, any 4-fermion charged current process may be written in terms of the effective vertex

$$\mathcal{M}^{CC} = \frac{1}{2 \sin \theta_w} \cdot \frac{-s}{q^2 + \cos^2 \theta_w M_Z^2 - i \text{Im} \Pi_{WW}^{1\text{-loop}}(q^2)} \cdot \frac{1}{\sin \theta_w} \quad (2.18)$$

We have inserted the tree level W width so that this expression remains finite on

W resonance. In the case in which only light quarks and leptons can be produced there we have¹²

$$\begin{aligned}
Im\Pi_{WW}^{1\text{-loop}}(-c_\theta^2 M_Z^2) &\equiv \Gamma_W^0 M_Z \cos \theta_w \\
&= \sum_{\substack{\text{fermions} \\ \text{pairs } f, f'}} \frac{\alpha M_Z^2 c_\theta^2}{12s_\theta^2} |U_{ff'}|^2 \left[1 - \frac{1}{2}(\delta_f + \delta_{f'}) + \frac{1}{2}(\delta_f - \delta_{f'})^2\right] \\
&\quad \times \left[1 - 2(\delta_f + \delta_{f'}) + (\delta_f - \delta_{f'})^2\right]^{1/2} \cdot C_{QCD}
\end{aligned} \tag{2.19}$$

where $\delta_f = m_f^2/c_\theta^2 M_Z^2$, $m_f + m_{f'} < M_W$ and $U_{ff'}$ is a Kobayashi-Maskawa quark mixing matrix element. Using the methods of this section it is easy to show that the 1-loop oblique corrections to (2.18) are

$$\begin{aligned}
\mathcal{M}^{CC}(q^2) &= \frac{1}{2\sin^2 \theta_w} (-s) \\
&\quad \times \left[(1 - 0.06) [(q^2 + \cos^2 \theta_w M_Z^2)(1 - \Delta_W(0)) \right. \\
&\quad \left. + \cos^2 \theta_w M_Z^2 \cdot \Delta_W(q^2)] - i Im\Pi_{WW}^{1\text{-loop}}(q^2) \right]^{-1}
\end{aligned} \tag{2.20}$$

where $\Delta_W(q^2)$ is obviously finite:

$$\Delta_W(q^2) = \Delta_W(-M_W^2) + \text{Re} \left(\frac{\Pi_{WW}(-M_W^2) - \Pi_{WW}(q^2)}{M_W^2} \right) \tag{2.21}$$

with

$$\begin{aligned}
\Delta_W(-M_W^2) &= -\frac{1}{\sin^2 \theta_w} \Delta_p(-M_Z^2) + \text{Re} \Delta_\alpha(-M_Z^2) - 0.06 - \frac{4\pi\alpha}{\sin^2 \theta_w \cos^2 \theta_w} \\
&\quad \times \frac{\text{Re}}{M_Z^2} \left(\Pi_{11}(-M_W^2) - \Pi_{11}(0) - \cos^2 \theta_w \Pi_{3Q}(-M_Z^2) \right).
\end{aligned} \tag{2.22}$$

This is the fourth and last function needed to discuss the effects of oblique corrections; it corresponds to the fourth possible vector self energy correction, the

W-W. It is clear from (2.20) that there are no oblique corrections to charged current processes at $q^2 = 0$ because we have used such a process, muon decay, to define one of the input parameters in our renormalization scheme. The position of the pole of the effective charged current vertex gives the W mass and we recover the result for *oblique* corrections

$$M_W^2 = M_Z^2 c_\theta^2 (1 + \Delta_W(-M_W^2)) . \quad (2.23)$$

The formula for the W^\pm mass shift was first written for GSW by Sirlin^{3, #1} and later by others.¹⁴ Again, it is simple to include direct corrections of vertices, fermion self-energies and boxes in charge current processes. We have, in analogy with (2.17), the finite quantity

$$\Gamma_+^{e\nu_e W} = \tilde{\Gamma}_+^{e\nu_e W} + \frac{1}{2} \left[A_+^e + 2m_e^2 \frac{\partial}{\partial p^2} (C^e - A_+^e) \right]_{p^2=-m_e^2} + \frac{1}{2} A_+^{\nu_e}(0) \quad (2.24)$$

where the 1PI charged vertex part is defined in Fig. 6. The effective charged current matrix element is defined so that it requires no radiative corrections, either oblique or direct, at $q^2 = 0$ since we use muon decay as an input parameter. Care has to be taken to transmit the direct corrections of muon decay into the neutral current and charged current matrix elements $M_{PP'}$ and M^{CC} . We call the reader's attention to the one-loop box diagrams contributing to muon decay depicted in Fig. 7 and the definition of the form factor $V_{++}^{\nu_\mu \mu e \nu_e}$. These are UV

#1 In GSW $\Delta_W(-M_W^2)$ is related to Sirlin's Δr for the W^\pm mass shift by

$$\Delta_W(-M_W^2) = \frac{-s_\theta^2}{\cos 2\theta_w} (\Delta r_{\text{vac. pol}} - 0.06)$$

finite and will contribute to both the shift in the W^\pm mass and to the various asymmetries in $e^+e^- \rightarrow \mu^+\mu^-, \tau^+\tau^-$. Also, we have to be very careful to include those QED corrections which are traditional in the definition of G_μ from τ_μ^{-1} in Eq. (1.2) throughout.

Thus, all one-loop corrections to neutral and charged current processes in $SU_2 \times U_1$ can be boiled down to the calculation of the following combinations of 1PI parts

1. oblique corrections:

$\Delta_W, \Delta_p, \Delta_\alpha, \Delta_\rho$ are combinations of vacuum polarization amplitudes.

2. direct corrections:

(a) box diagrams are UV finite

(b) vertex parts $\Gamma_\pm^{ffZ}, \Gamma_\pm^{ffA}, \Gamma_+^{ff'W}$ are combinations of 1PI vertex parts and self energies of fermions f, f' .

These are inserted into effective matrix elements for neutral $\mathcal{M}_{PP'}$ and charged \mathcal{M}^{CC} current processes. All cross section to one loop are just functions of \mathcal{M}^{CC} and $\mathcal{M}_{PP'}$ apart from kinematics.

In the next section we will define some physically measurable quantities, mostly on Z^0 resonance $q^2 = -M_Z^2$, and display the GSW one-loop corrections to them. In Section 4 we will give the response of these quantities to new physics, mostly obliquely coupled; e.g. extra quarks and leptons, SUSY, technicolor, etc.

3. Measurables: Response to One-loop in GSW

In the last section we saw that all one-loop corrections in $SU_2 \times U_1$ could be incorporated into effective matrix elements for neutral current \mathcal{M}_{PP} , and charged-current \mathcal{M}^{CC} four-fermion processes if the masses of external fermions were small. In this section we will define a number of physical measurables and give the response of these to one-loop corrections in the standard GSW model with three generations of quarks and leptons. All of the results of this section are from the work of Lynn and Stuart^{5,11} whose computer program calculates all four-fermion processes to one-loop in GSW excluding the graphs of Fig. 2.

Let us start with the various asymmetries in $e^+e^- \rightarrow \mu^+\mu^-$ or $\tau^+\tau^-$. These are obviously given by various combinations of the cross sections (2.1). We first discuss the calculation of the initial state longitudinal polarization asymmetry in lepton pair production. This quantity is defined as:

$$A_{LR} = \frac{\sigma(e^-(L)e^+ \rightarrow \ell^-\ell^+) - \sigma(e^-(R)e^+ \rightarrow \ell^-\ell^+)}{\sigma(e^-(L)e^+ \rightarrow \ell^-\ell^+) + \sigma(e^-(R)e^+ \rightarrow \ell^-\ell^+)}. \quad (3.1)$$

We begin by examining the longitudinal polarization asymmetry, A_{LR} , because it will be shown that of the available asymmetries in $e^+e^- \rightarrow \mu^+\mu^-$ on Z^0 resonance it is the most sensitive to radiative corrections. The shifts in the forward-backward asymmetry, A_{FB} , and transverse polarization asymmetry A_{\perp} due to higher order corrections can be expressed in terms of the shift in A_{LR} . Hence no new information is available from them. It should be borne in mind that initial state longitudinal polarization will not be available in the early stages of LEP. However the observed sensitivity is presented as a strong argument for its eventual inclusion. Also, a careful measurement of the τ^- final state longi-

nal polarization asymmetry (defined below) is equally sensitive to the effects of radiative corrections and should be a higher priority at LEP.

Unless otherwise stated we will assume, because we are primarily interested in LEP/SLC physics, that the energy of the reaction $e^+e^- \rightarrow \mu^+\mu^-, \tau^+\tau^-$ is tuned precisely to the Z^0 resonance; then the Z propagator is purely imaginary, so that not only does the diagram with a Z^0 in the s -channel dominate, but (modulo the imaginary parts of 1PI vertex and self-energy parts) there are also no interference terms with the photon exchange diagram. The contribution of the photon exchange diagram to the cross section is $\sim 10^{-2}$ times that of the Z^0 exchange diagram and so we will concentrate primarily on corrections to the Z^0 pole part.

At leading order in perturbation theory, A_{LR} on resonance is given precisely by the asymmetry in the couplings of $e(L)$ and $e(R)$ to the Z^0 :

$$\begin{aligned} A_{LR}|_0 &= \frac{(\frac{1}{2} - \sin^2 \theta_w)^2 - (\sin^2 \theta_w)^2}{(\frac{1}{2} - \sin^2 \theta_w)^2 + (\sin^2 \theta_w)^2}, \\ &= \frac{-2v_\theta}{1 + v_\theta^2}, \end{aligned} \tag{3.2}$$

where $v_\theta = (4 \sin^2 \theta_w - 1)$. Let us now define:

$$\delta A_{LR} = A_{LR} - A_{LR}|_0, \tag{3.3}$$

where $A_{LR}|_0$ is to be evaluated using (1.4). δA_{LR} is directly measurable, in the sense that it may be computed directly from the physical quantities α , G_μ , M_Z , and A_{LR} . We have argued above that the indicated difference can eventually be measured to a few tenths of a percent by precision experiments¹ at the Z^0 .

Our main focus, then, will be on assessing the size of the difference δA_{LR} to be expected in a variety of models of physics.

To clarify the situation, let us for the moment consider only oblique corrections (gauge boson vacuum polarization amplitudes) and, of these, only those entering the Z^0 exchange part of $M_{PP'}$. Then we find that^{6,11,15}

$$\begin{aligned}
\delta A_{LR}^{\text{oblique}} &= -8 \cdot \frac{1 - v_\theta^2}{(1 + v_\theta^2)^2} \cdot \Delta_p(-M_Z^2) \\
&= 64 \frac{\sin^2 \theta_w}{(1 + v_\theta^2)^2} \cdot 4\pi\alpha \frac{\text{Re}}{M_Z^2} \left[-\Pi_{11}(0) + \Pi_{33}(-M_Z^2) - \Pi_{3Q}(-M_Z^2) \right. \\
&\quad \left. + \cos^2 \theta_w \sin^2 \theta_w \left[\Pi_{QQ}(-M_Z^2) + M_Z^2 \Pi_{QQ}'(0) + 0.06 \frac{M_Z^2}{4\pi\alpha} \right] \right].
\end{aligned} \tag{3.4}$$

Thus, A_{LR} is only sensitive on Z^0 resonance to the quantity $\Delta_p(-M_Z^2)$ for oblique corrections. In adding direct corrections, we must be careful about two sources. Those from muon decay used to define our input parameter G_μ will just be added on to $\Delta_p(-M_Z^2)$ since they effectively only change the value of $\sin^2 \theta_w$ when included.³ Direct correction to the electron- Z^0 vertex will appear, since this is a left-right asymmetry, in the combination $\Gamma_+^{eez} - \Gamma_-^{eez}$. We have excluded the QED detector dependent graphs⁹ of Fig. 2, the neutral current boxes do not have the correct Z^0 pole structure to contribute heavily and Γ_Z drops out in the *ratio* of cross sections. Thus, including only the Z^0 pole terms we have¹⁵

$$\begin{aligned}
\delta A_{LR} = & -8 \frac{1 - v_\theta^2}{1 + v_\theta^2} \Delta_p(-M_Z^2) - \frac{64 s_\theta^4 c_\theta^2}{(1 + v_\theta^2)^2} \\
& \times \left\{ \Gamma_+^{e\nu_e w}(0) + \Gamma_+^{\mu\nu_\mu w}(0) + \left(\frac{1 - 2s_\theta^2}{c_\theta} \right)^2 \right. \\
& \left. \times \left(\Gamma_-^{eez}(-M_Z^2) - \Gamma_+^{eez}(-M_Z^2) \right) + V_{++}^{\nu_\mu \mu \nu_e}(0) \right\} \quad (3.5)
\end{aligned}$$

where the Γ 's are effective vertex parts depicted in Figs. 4, 5 and 6 and Eqs. (2.17) and (2.24) and $V_{++}^{\nu_\mu \mu \nu_e}(0)$ are the box diagrams from muon decay depicted in Fig. 7 evaluated with zero external momenta.^{‡2} All of the one-loop GSW corrections to A_{LR} except those of Fig. 2 have been calculated by Lynn and Stuart (and later by Hollik¹⁶), including corrections to photon exchange, boxes and a careful treatment of the various imaginary parts of one-loop vertex and self-energies. The results are given in Table I and, indeed, the above corrections are dominant. Notice the dramatic dependence of A_{LR} on the precise values of M_Z relative to $G_\mu^{-\frac{1}{2}}$ as well as a large Higgs and top quark masses. In order to make a sensible (to us at least) statement about the size of the GSW weak corrections due to internal gauge bosons, etc., which are *not* taken into account by the QED renormalization of α from $q^2 = 0$ to $-M_Z^2$ we display the quantity

$$\begin{aligned}
\delta A_{LR}^{\text{GSW}}(m_t = 30, m_H = 100) &= A_{LR}(m_t = 30, m_H = 100) - A_{LR}|_0 \\
&= - \left\{ \begin{array}{c} 0.0257 \\ 0.0242 \\ 0.0237 \end{array} \right\} \text{ for } M_Z = \left\{ \begin{array}{c} 90 \\ 94 \\ 98 \end{array} \right\} \text{ GeV} . \quad (3.6)
\end{aligned}$$

Here, all masses are in GeV. Thus, GSW weak corrections are measurable in the

^{‡2} In (3.5) we have not displayed the QED corrections traditional in the definition (1.2) of G_μ . They are, of course, included in our numerical evaluations throughout this section.

initial state longitudinal polarization asymmetry.¹ Further, we see the variation with large top quark mass and Higgs' mass

$$\delta A_{LR}^{GSW}(m_t = 180, m_H = 100, M_Z = 94) = -0.0242 + 0.0294 \quad (3.7)$$

$$\delta A_{LR}^{GSW}(m_t = 30, m_H = 1000, M_Z = 94) = -0.0242 - 0.009. \quad (3.8)$$

The next quantity to be examined is the forward-backward asymmetry, which for 2 particle final states is the same as the charge asymmetry:

$$A_{FB} = \frac{\int d\phi \left[\int_0^1 - \int_{-1}^0 \right] d \cos \theta \frac{d\sigma}{dt} (e^+e^- \rightarrow f\bar{f})}{\int d\phi \left[\int_0^1 + \int_{-1}^0 \right] d \cos \theta \frac{d\sigma}{dt} (e^+e^- \rightarrow f\bar{f})}. \quad (3.9)$$

For a fermion of charge Q and left-handed isospin I_3 , the zeroth-order formula for the this asymmetry on Z^0 resonance is:

$$A_{FB}^f|_0 = \frac{3}{4} \left(\frac{-2v_\theta}{1 + v_\theta^2} \right) \left(\frac{2I_L^3 a_f}{a_f^2 + I_3^2} \right), \quad (3.10)$$

where

$$a_f = I_L^3 - 2Q \sin^2 \theta_w \quad (3.11)$$

with left-handed weak isospin component I_L^3 for the fermion. The forward-backward asymmetry in GSW including all one-loop corrections except those of Fig. 2 is given in Table II from the work of Lynn and Stuart. It has also been calculated in GSW by many others.¹⁶ We note that it is dramatically dependent on the precise value of M_Z . This is easy to understand since at tree level $A_{FB} \simeq 3v_\theta^2$ on Z^0 resonance and small shifts in s_θ^2 away from 1/4 give large

shifts in $v_\theta = 4 \sin^2 \theta_w - 1$. If we define the shifts from the calculated value in analogy with (3.6)

$$\delta A_{FB}^{GSW} = A_{FB}^{GSW} - A_{FB}|_0 \quad (3.12)$$

then the GSW weak corrections are

$$\delta A_{FB}^{GSW}(m_H = 30, m_H = 100) = - \begin{Bmatrix} 0.0008 \\ 0.0076 \\ 0.0123 \end{Bmatrix} \quad \text{for } M_Z = \begin{Bmatrix} 90 \\ 94 \\ 98 \end{Bmatrix} \quad (3.13)$$

and the response to heavy top quarks and Higgs' are

$$\delta A_{FB}^{GSW}(m_t = 180, m_H = 100, M_Z = 94) = -0.0076 + 0.0075 \quad (3.14)$$

$$\delta A_{FB}^{GSW}(m_t = 30, m_H = 1000, M_Z = 94) = -0.0076 - 0.0038 . \quad (3.15)$$

The charge asymmetry is less sensitive to the effects of radiative corrections than is the left-right longitudinal polarization asymmetry. This is easily understood from (2.4) as follows. On Z^0 resonance the shift due to oblique corrections in the charge asymmetry or any other asymmetry or cross section in $e^+e^- \rightarrow f\bar{f}$, with $f \neq e, \nu_e$ a light fermion depends only on I_3 , Q and the particular combination $\Delta_p(-M_Z^2)$; this is essentially only a statement about the dominance of the Z^0 exchange graph for neutral current processes on resonance. Using the methods of the last section, one may easily show that the shifts in this asymmetry is for final state fermions f

$$\delta A_{FB}^f \simeq \frac{3I_L^3}{2((I_L^3)^2 + a_f^2)} \cdot \left(a_f + \frac{v_\theta Q}{2} \frac{1 + v_\theta^2 a_f^2 - (I_L^3)^2}{1 - v_\theta^2 a_f^2 + (I_L^3)^2} \right) \cdot \delta A_{LR} \quad (3.16)$$

in the case in which the Z^0 pole terms only are included. Since $a_\mu = v_\theta/2$ both terms on the right-hand side are suppressed by v_θ for the charge asymmetry in

$e^+e^- \rightarrow \mu^+\mu^-$. In fact, since at tree level on Z^0 resonance

$$A_{FB}^\mu|_0 = \frac{3}{4} (A_{LR}|_0)^2 \quad (3.17)$$

we have

$$\delta A_{FB}^\mu \simeq \frac{3}{2} A_{LR}|_0 \cdot \delta A_{LR} = -\frac{3v_\theta}{1+v_\theta^2} \cdot \delta A_{LR} \quad (3.18)$$

including both oblique and direct corrections if $\mu - e$ universality is assumed.

This suppression (especially for small M_Z) by a factor of v_θ of the contribution of new heavy oblique particles is true for *any* asymmetry formed from $e^+e^- \rightarrow \mu^+\mu^-$, $\tau^+\tau^-$ on Z^0 resonance in which the longitudinal polarization of incoming or outgoing particles is unobserved. *Thus the capacity for longitudinal polarization measurement in leptonic processes on Z^0 resonance is crucial for the observation of small effects due to radiative corrections in GSW.*

Anticipating the possibility of obtaining transverse polarization on both the $e^+(P_\perp^+)$ and $e^-(P_\perp^-)$ beams at LEP, we may define the transverse or azimuthal (ϕ) asymmetry A_\perp on Z^0 resonance

$$A_\perp = \frac{4}{P_\perp^+ P_\perp^-} \frac{\int d\Omega \cos 2\phi \frac{d\sigma}{dt} (e^+e^- \rightarrow \mu^+\mu^-)}{\int d\Omega \frac{d\sigma}{dt} (e^+e^- \rightarrow \mu^+\mu^-)} \quad (3.19)$$

The GSW one-loop calculations of Lynn and Stuart for this quantity excluding the graphs of Fig. 2 are given in Table III. From the lowest order Z^0 resonance formula

$$A_\perp|_0 = \frac{v_\theta^2 - 1}{v_\theta^2 + 1} \quad (3.20)$$

we may display the shifts due to the one-loop weak corrections in analogy with

(3.6)

$$\delta A_{\perp}^{GSW}(m_t = 30, m_H = 100) = \begin{Bmatrix} 0.0103 \\ 0.0043 \\ 0.0007 \end{Bmatrix} \quad \text{for } M_Z = \begin{Bmatrix} 90 \\ 94 \\ 98 \end{Bmatrix} \text{ GeV} \quad (3.21)$$

As well as large top and Higgs' masses

$$\delta A_{\perp}^{GSW}(m_t = 180, m_H = 100, M_Z = 94) = 0.0043 + 0.0036 \quad (3.22)$$

$$\delta A_{\perp}^{GSW}(m_t = 30, m_H = 1000, M_Z = 94) = 0.0043 - 0.0026 . \quad (3.23)$$

Note that the response of A_{\perp} to radiative corrections is also a lot smaller than that of A_{LR} . In fact we may easily show from examination of the tree-level formula and the methods of the previous section that

$$\delta A_{\perp} \simeq \frac{-2v_{\theta}}{1 - v_{\theta}^2} \delta A_{LR} \simeq \frac{2}{3} \delta A_{FB}^{\mu} \quad (3.24)$$

when only Z^0 pole terms are taken into account for both direct and oblique corrections.

We now indicate why this suppression by $v_{\theta} = 4s_{\theta}^2 - 1$ occurs for radiative corrections on Z^0 pole for *any* asymmetry in $e^+e^- \rightarrow \mu^+\mu^-, \tau^+\tau^-$ in which the longitudinal polarization is not observed. Such an asymmetry, at tree level, must be only a function of the quantity

$$\left(\frac{\ell^+ \text{ vector coupling to } Z^0}{\ell^+ \text{ axial vector couplings to } Z^0} \right)^2 = v_{\theta}^2 . \quad (3.25)$$

From (2.4) and (3.5) we can see that the effect of radiative corrections on Z^0

pole exchange diagrams is to displace

$$s_\theta^2 \rightarrow s_\theta^2 + \Delta_p(M_Z^2) + \frac{s_\theta^2 c_\theta^2}{1 - 2s_\theta^2} \times \left\{ \Gamma_+^{e\nu_e w}(0) + \Gamma_+^{\mu\nu_\mu w}(0) + \left(\frac{1 - 2s_\theta^2}{c_\theta} \right)^2 (\Gamma_-^{eez}(-M_Z^2) - \Gamma_+^{eez}(-M_Z^2)) + V_{++}^{\nu_e e \nu_e}(0) \right\} \quad (3.26)$$

if $\mu - e - \tau$ universality is obeyed. Thus, the shift in any asymmetry A without longitudinal polarization in $e^+e^- \rightarrow \mu^+\mu^-, \tau^+\tau^-$ is

$$\delta A = (\text{const})v_\theta \delta v_\theta = (\text{const}')v_\theta \delta A_{LR} . \quad (3.27)$$

This suppression by a factor v_θ is especially disastrous for small M_Z and makes the observation of small effects due to radiative corrections extremely difficult in asymmetries formed without the observation of longitudinal polarization. Asymmetries with longitudinal polarization on Z^0 resonance escape this argument because they are, at tree level, functions only of v_θ rather than v_θ^2 . Thus, the shifts due to radiative corrections in asymmetries with the observation of longitudinal polarization $\sim \delta v_\theta$ and so avoid the suppression factor.

One asymmetry whose response to radiative corrections is therefore not suppressed by the factor v_θ is the τ^- polarization asymmetry on Z^0 resonance.

$$A_{\tau_{\text{pol}}} = \frac{\sigma(e^+e^- \rightarrow \tau^+\tau^-_L) - \sigma(e^+e^- \rightarrow \tau^+\tau^-_R)}{\sigma(e^+e^- \rightarrow \tau^+\tau^-_L) + \sigma(e^+e^- \rightarrow \tau^+\tau^-_R)} . \quad (3.28)$$

On Z^0 resonance in $SU_2 \times U_1$ (leaving aside the question of hadronization of the τ^- decay products and the graphs of Fig. 2) we have

$$A_{\tau_{\text{pol}}} = A_{LR} \quad (3.29)$$

so that this too can be read off from Table II. The τ^- polarization asymmetry

would in principle provide a good test of the one-loop radiative corrections and should be a high priority at LEP/SLC.

For completeness, we display A_{FB} and A_{LR} as functions of the center-of-mass energies \sqrt{s} in Figs. 8 and 9. The dashed lines include no radiative corrections, *not even the 0.06 QED correction inserted in our Born terms s_0^2 in Eq. (1.4)*. The solid lines include all GSW corrections except those of Fig. 2 for $m_t = 30$ and $m_H = 100$. The dotted line in Fig. 9 includes the 0.06 from the “trivial” QED correction in the definition of $\sin^2 \theta_w$ given in Eq. (1.4) and shows that the bulk of the shift is indeed due to this. Remember though that the observation of this shift would indicate that some sort of unification picture of weak and electromagnetic interactions is correct but it would not indicate which particular gauge group is demanded.

Let us now make use of our complete expression for \mathcal{M} to analyze Bhabha scattering. In terms of the functions introduced in (2.4), the Bhabha scattering cross-section, including 1-loop corrections, is given by

$$\begin{aligned} \frac{d\sigma}{dt}(e^-(L)e^+ \rightarrow e^+e^-) &= \frac{4\pi\alpha^2}{s} \left\{ |\mathcal{M}_{LL}(-s) + \mathcal{M}_{LL}(-t)|^2 k_{LL}^2 \right. \\ &\quad \left. + |\mathcal{M}_{LR}(-s)|^2 k_{LR}^2 + |\mathcal{M}_{LR}(-t)|^2 \right\} \end{aligned} \quad (3.30)$$

$$\begin{aligned} \frac{d\sigma}{dt}(e^-(R)e^+ \rightarrow e^+e^-) &= \frac{4\pi\alpha^2}{s} \left\{ |\mathcal{M}_{RR}(-s) + \mathcal{M}_{RR}(-t)|^2 k_{RR}^2 \right. \\ &\quad \left. + |\mathcal{M}_{RL}(-s)|^2 k_{RL}^2 + |\mathcal{M}_{RL}(-t)|^2 \right\} \end{aligned} \quad (3.31)$$

At the Z^0 resonance, the cross-section is dominated over the whole range of t by the contributions of the Z in the s -channel and the photon in the t -channel.

The relative size of these two contributions is a strong function of t : The photon term dominates near zero angle θ (the angle between incoming and outgoing electrons) the Z at 90° . The two terms are roughly equal for $\cos\theta \simeq 0.8$. If, then, we consider the polarization asymmetry in Bhabha scattering near 90° , we are measuring exactly the same correction that we have found already in the μ and τ polarization or charge asymmetries. We should investigate whether Bhabha scattering can also give new, independent information on weak radiative corrections.

New information about one-loop radiative corrections might come from the first term in (2.4) in the t -channel in forward or near forward directions. However, because we used $\alpha(q^2 = 0)$ as an input parameter, the renormalization will engineer itself so that radiative corrections will disappear at $t = 0$, the far forward direction, in the photon exchange graph. Our only hope, then, to see effects of radiative corrections in Bhabha scattering not already contained in $e^+e^- \rightarrow \mu^+\mu^-$ is in the *endcap* region $\cos\theta \sim 0.8$ when $\sqrt{-t} \sim 30$ GeV. Thus, one might hope to observe new effects in Bhabha scattering in the near-forward direction. GSW radiative corrections to Bhabha scattering have been calculated by many authors.¹⁷ There is one subtlety in the measurement however because Bhabha scattering is used in the forward direction to calibrate the luminosity in the first place. The luminosity (which usually suffers a rather large systematic error $\sim 5\%$ for our purposes) is only necessary for the measurement of an absolute cross section so that we should study a ratio of cross sections in order to see small effects clearly. Let us define the quantity:

$$X = \left(\frac{\frac{d\sigma}{dt}(e^+e^- \rightarrow e^+e^-)}{\frac{d\sigma}{dt}(e^+e^- \rightarrow \mu^+\mu^-)} - 1 \right)_{s=M_Z^2} \cdot (1 - \cos\theta)^2. \quad (3.32)$$

This and all other four lepton processes have been calculated to one-loop in GSW by Lynn and Stuart excluding the graphs of Fig. 2. Their results are displayed as a function of $\cos \theta$ in Table IV. The large shift in X as the top quark mass changes from 30 to 180 GeV is primarily due to the diminishment of the Z^0 width (X is proportional to Γ_Z^2) as the top becomes too heavy to produce on Z^0 resonance. Radiative corrections to X in the near-forward and forward direction are small because radiative corrections to the Z^0 width tend to be small as we shall see below.

Off Z^0 resonance we may hope to exploit the $Z - A$ interference terms in the endcap region in Bhabha scattering or by studying μ pair production to get information about the new quantity Δ_ρ . This new information would also be in the *shape* of the cross sections in $e^+e^- \rightarrow \mu^+\mu^-$ with or without polarization as one scans across the Z^0 resonance. Let us examine the corrections to the Z^0 width Γ_Z . To relative $O(\alpha)$ the definition of the width is subtle because it is extracted experimentally by studying the shape of the resonance; we define it by writing the one-loop Z^0 propagator near the Z^0 pole as

$$G_Z \rightarrow \frac{Z_Z}{q^2 + M_Z^2 - i\Gamma_Z M_Z - i\epsilon} \quad (3.33)$$

so that including oblique corrections

$$\Gamma_Z = \Gamma_Z^0 \cdot (1 - C_\Gamma \Delta_\rho(-M_Z^2) + \Delta_\rho(-M_Z^2) + 0.06) . \quad (3.34)$$

Note that, as expected, the Z^0 width involves the first derivative of the Z^0 self energy on resonance through the parameter Δ_ρ . Oblique corrections to the imaginary part of the Z^0 inverse propagator are due to the shifts in the coupling

constants and the appropriate part of the $Z - A$ mixing^{‡3}; the same sources of shift as in the polarization asymmetry. Therefore the Z^0 width is corrected by the *same* function $\Delta_\rho(-M_Z^2)$ as is the polarization asymmetry. The constant C_Γ is easily calculated from these considerations:

$$C_\Gamma = \frac{\partial}{\partial s_\theta^2} \ln(c_\theta^2 s_\theta^2 \Gamma_Z^0). \quad (3.35)$$

In the case in which only light fermions can be created on Z^0 resonance,

$$C_\Gamma =$$

$$\frac{\sum_{\text{fermions}} Q(I_L^3 - 2Q \sin^2 \theta_w) \left(1 + \frac{2m_f^2}{M_Z^2}\right) \left(1 - \frac{4m_f^2}{M_Z^2}\right)^{1/2} C_{QCD}}{\sum_{\text{fermions}} \left[\left(\frac{I_L^3}{2} - Q \sin^2 \theta_w\right)^2 \left(1 + \frac{2m_f^2}{M_Z^2}\right) + \left(\frac{I_L^3}{2}\right)^2 \left(1 - \frac{4m_f^2}{M_Z^2}\right) \right] \left(1 - \frac{4m_f^2}{M_Z^2}\right)^{1/2} C_{QCD}} \quad (3.36)$$

where $C_{QCD} = 1$ for leptons and $3 \cdot \left(1 + \frac{\alpha_{\text{strong}}(-M_Z^2)}{\pi}\right)$ for quarks. For 3 light $m_f^2 \ll M_Z^2$ generations of quarks and leptons, $C_\Gamma \rightarrow 1$ as $s_\theta^2 \rightarrow 1/4$. Also $\Delta_\rho(-M_Z^2)$ is small in GSW so that including oblique corrections

$$\Gamma_Z \simeq \Gamma_Z^0 \left(1 + \frac{1}{8} \delta A_{LR}^{\text{oblique}} + 0.06\right). \quad (3.37)$$

Thus shifts in the Z^0 width from radiative corrections tend to be small. The Z^0 width has been calculated by Lynn and Stuart including all GSW corrections to one loop, with the proviso that fermion masses are small in 1PI one-loop vertex parts only (helicity conserving vertices). In particular, the top quark mass and associated Higgs' exchange graphs have been neglected within one-loop 1PI

^{‡3} In the case of direct-coupling theories we need to include the imaginary part of the 2-loop Z^0 self energy.

fermion self-energies and vertex parts but have been included in vector boson self-energies and in (2.3). This may be a bad idea for heavy t quarks and a more complete calculation should be done. Also, all strong interaction corrections are neglected. These results, displayed in Table V, show that Γ_Z is a strong function of the precise Z^0 mass $\Gamma_Z \sim G_\mu M_Z^3$ and of whether the top quark is light enough to be produced on resonance. All GSW effects in Γ_Z , especially the creation of b and t quarks (which involves Higgs' exchange in internal loops because for large top mass the Yukawa couplings are large) and toponium (if recent CERN reports on the t quark mass are vindicated) must be clearly understood before this quantity is used to count neutrino species. We note that this requires knowledge of the strong interactions.

Next, let us examine the GSW radiative corrections to the precise W^\pm mass.¹⁴ This was of course first calculated to one-loop by Sirlin³ and later by Consoli *et. al.*¹⁴ An independent check was then done by Lynn and Stuart whose results appear in Table VI. We note the strong dependence on Z , top and Higgs' masses. To see the effects of weak GSW corrections clearly we form the quantity

$$\delta M_W = M_W - c_\theta M_Z \quad (3.38)$$

‡4 Besides the QED corrections traditional in the definition (1.2) for G_μ , Sirlin's formula for the GSW shift reads in our notation

$$\Delta r - 0.06 = \left[\Gamma_+^{e\nu e w}(0) + \Gamma_+^{\mu\nu\mu w}(0) + V_{++}^{\nu\mu\mu e\nu e}(0) - \frac{1 - 2s_\theta^2}{s_\theta^2} \Delta_W(-M_W^2) \right]_{GSW} + QED \text{ corrections} .$$

$$\delta M_W^{GSW}(m_t = 30, m_H = 100) = - \left\{ \begin{array}{c} 170 \\ 180 \\ 170 \end{array} \right\} \text{ MeV} \quad \text{for } M_Z = \left\{ \begin{array}{c} 90 \\ 94 \\ 98 \end{array} \right\} \text{ GeV} . \quad (3.39)$$

To see the effects of heavy top and Higgs' masses we display the shifts

$$\delta M_W^{GSW}(m_t = 180, m_H = 100, M_Z = 94) = (-180 + 780) \text{ MeV} \quad (3.40)$$

$$\delta M_W^{GSW}(m_t = 30, m_H = 1000, M_Z = 94) = (-180 - 160) \text{ MeV} . \quad (3.41)$$

A precise determination of the W^\pm mass must be a high priority at LEP2 which will have enough energy to produce W 's in pairs via $e^+e^- \rightarrow W^+W^-$.

In analogy to the Z^0 width (3.33) we define the W^\pm width by writing the propagator near the W^\pm pole as

$$G_W \rightarrow \frac{Z_W}{q^2 + M_W^2 - i\Gamma_W M_W - i\epsilon} \quad (3.42)$$

so that including only oblique corrections

$$\Gamma_W = \Gamma_W^0 \left[1 + 0.06 + \frac{1}{2} \Delta_W(-M_W^2) + \Delta_W(0) + q^2 \frac{\partial}{\partial q^2} \Delta_W(q^2) \Big|_{q^2=-M_W^2} \right] . \quad (3.43)$$

We do not display the one-loop GSW results for Γ_W here^{11,14} but note only that it also is a strong function ($\Gamma_W \sim G_\mu M_W^3$) of M_Z .

Finally, we should compare the information from high energy LEP/SLC experiments on radiative corrections to that from low energy data, say, $\nu_\mu e$ scattering¹⁸ from the CHARM II collaboration. It is easy to write down the cross sections—all in the t channel—for the three processes $\nu_\mu e \rightarrow \nu_\mu e$, $\bar{\nu}_\mu e \rightarrow \bar{\nu}_\mu e$ and

$\nu_\mu e \rightarrow \nu_e \mu$ in terms of the effective matrix elements $\mathcal{M}_{PP'}$ and \mathcal{M}^{CC} . Again, because we worry about the neutrino beam luminosity, we will form only ratios of cross sections:

$$R_{\nu\bar{\nu}} = \frac{\sigma(\nu_\mu e \rightarrow \nu_\mu e)}{\sigma(\bar{\nu}_\mu e \rightarrow \bar{\nu}_\mu e)} = \frac{|\mathcal{M}_{\nu_L e_L}(-t)|^2 + \frac{1}{3} |\mathcal{M}_{\nu_L e_R}(-t)|^2}{\frac{1}{3} |\mathcal{M}_{\nu_L e_L}(-t)|^2 + |\mathcal{M}_{\nu_L e_R}(-t)|^2} \quad (3.44)$$

$$R_{NC;CC} = \frac{\sigma(\nu_\mu e \rightarrow \nu_\mu e)}{\sigma(\nu_\mu e \rightarrow \nu_e \mu)} = \frac{|\mathcal{M}_{\nu_L e_L}(-t)|^2 + \frac{1}{3} |\mathcal{M}_{\nu_L e_R}(-t)|^2}{|\mathcal{M}^{CC}(-t)|^2 \cdot \left(1 - \frac{m_\mu^2}{2m_e E_\nu}\right)^2}. \quad (3.45)$$

In (3.44) and (3.45) we have assumed t small enough so as to neglect the $\cos \theta$ dependence in the Z , W propagators. We have also neglected a slight $\cos \theta$ dependence in the box and vertex diagrams and have written $R_{NC;CC}$ in the target electron rest frame. The largest part of the effects of radiative corrections can be read off from (2.4) by considering only the *oblique* corrections

$$R_{\nu\bar{\nu}} \simeq \left(1 - \frac{\hat{v}_\theta}{1 + \hat{v}_\theta^2}\right) \bigg/ \left(1 + \frac{\hat{v}_\theta}{1 + \hat{v}_\theta^2}\right) \quad (3.46)$$

$$R_{NC;CC} \simeq \frac{1 - \hat{v}_\theta + \hat{v}_\theta^2}{12} (1 - \Delta_\rho(-t))^{-2} \left(1 - \frac{m_\mu^2}{2m_e E_\nu}\right)^{-2} \quad (3.47)$$

$$\hat{v}_\theta = 4(s_\theta^2 + \Delta_p(-t)) - 1 \quad (3.48)$$

so that $R_{\nu\bar{\nu}}(t = 0)$ depends on the combination $\Delta_p(0)$ while $R_{NC;CC}(t = 0)$ depends on $\Delta_p(0)$ as well as $\Delta_\rho(t = 0)$. This confirms that these quantities measure radiative corrections which are different than those measured in experiments on Z^0 and W^\pm resonance which access primarily $\Delta_p(-M_Z^2)$ and $\Delta_W(-M_W^2)$. A complete calculation of all GSW radiative corrections (except the QED diagrams of Fig. 2) was done by Lynn and Stuart with no assumptions about $\cos \theta$ dependence. Their results are given in Tables VII and VIII. Note again the dependence

on the precise value of M_Z , m_t , m_H . Thus $R_{\nu\bar{\nu}}$ and $R_{NC;CC}$ can be used to eliminate a large fraction of the parameter space of the Tables. Then the various asymmetries in $e^+e^- \rightarrow \mu^+\mu^-$, $\tau^+\tau^-$ and the W^\pm mass can be used to give a clear test of GSW at the one-loop level.

We have now examined the results of one-loop radiative corrections due to the GSW theory. In the next section we will examine the response of various experimentally measurable quantities to corrections due to representations of new particles in $SU_2 \times U_1$ beyond GSW.

4. New Physics

In this section we examine the corrections to the various asymmetries in $e^+e^- \rightarrow \mu^+\mu^-$ and $\tau^+\tau^-$ on Z^0 resonance and to the W^\pm mass from new physics; that physics designed to “explain” the constant parameters in GSW. We will examine extra generations of quarks and leptons, SUSY and technicolor (not extended) contributions to one-loop. All of the results of this section are taken from the work of Lynn¹⁵ and Lynn and Peskin.⁶

For the asymmetries, we have shown that this can be reduced to the calculation of only δA_{LR} on Z^0 resonance with the others related by

$$\begin{aligned} \delta A_{FB}^\mu &\simeq \frac{-3v_\theta}{1+v_\theta^2} \delta A_{LR} \\ &\simeq \begin{Bmatrix} 0.12 \\ 0.44 \\ 0.68 \end{Bmatrix} \delta A_{LR} \quad \text{for } M_Z = \begin{Bmatrix} 90 \\ 94 \\ 98 \end{Bmatrix} \text{ GeV} \end{aligned} \tag{4.1}$$

$$\delta A_{\perp} \simeq \frac{-2v_{\theta}}{1-v_{\theta}^2} \delta A_{LR}$$

$$\simeq \begin{Bmatrix} 0.08 \\ 0.31 \\ 0.45 \end{Bmatrix} \delta A_{LR} \quad \text{for } M_Z = \begin{Bmatrix} 90 \\ 94 \\ 98 \end{Bmatrix} \text{ GeV} \quad (4.2)$$

$$\delta A_{\tau_{\text{pol}}} = \delta A_{LR} . \quad (4.3)$$

Note the numerical suppression of the longitudinally unpolarized asymmetries relative to those with longitudinal polarization, especially for low Z^0 masses. If M_Z turned out to be small (~ 90 GeV), we would have little hope of seeing the effects of one-loop radiative corrections in Z^0 resonance lepton asymmetries in which the longitudinal polarization of an initial or final state charged lepton were unobserved. *Thus the capacity for observation of longitudinal polarization is crucial for the observations of small effects on Z^0 resonance which could betray the existence of new particles.*

The astute reader will notice that these relations are not quite satisfied in the Tables I and II. This is due to the inclusion of certain *two-loop* effects in the numerical evaluations of A_{LR} and A_{FB} . We thus estimate that two-loop effects contribute to A_{FB} and A_{LR} at the level of about $\sim \pm 0.001$ and $\sim \pm 0.002$ respectively. These should be understood (with a lot of further work) before comparison with LEP/SLC data is to be made. Further, we note that the effects of hard and soft bremsstrahlung may have to be understood to $\mathcal{O}(\alpha^4)$ in the cross sections as well although most of these effects are expected to cancel in A_{LR} and A_{\perp} (but not in A_{FB}) as shown by Bohm and Hollik.⁹

If the standard model is modified in the region of a few hundred GeV, we must add to the contributions of GSW the contributions from new physics. To

facilitate this analysis, let us divide models of this new physics into two classes: those with *direct* and *oblique* couplings. The second class contains those models with no vertices linking the new particles present in the model with the three light families of quarks and leptons. The new particles then influence leptonic processes only indirectly, by means of their influence on the electroweak gauge bosons. Models with additional heavy quarks and leptons, and models, such as technicolor, which mainly modify the Higgs sector, have only these oblique couplings. Supersymmetric models, which postulate bosonic partners of the light fermions, and models with right-handed leptonic currents are directly coupled. However, even in these models, the partners of any quarks and new heavy leptons have only oblique couplings. As we have seen in the previous two sections, oblique theories are much easier to analyze, because they contribute to the basic process $e^+e^- \rightarrow \mu^+\mu^-$ only through vacuum polarization diagrams. Thus we have only to calculate

$$\delta A_{LR}^{\text{oblique}} = -64 \frac{\cos^2 \theta_w \sin^4 \theta_w}{(1 + v_\theta^2)^2} \text{Re} \left[\frac{\cos 2\theta_w}{\cos \theta_w \sin \theta_w} \frac{\Pi_{ZA}(-M_Z^2)}{M_Z^2} - \Pi_{AA}'(0) \right. \\ \left. + \frac{\Pi_{WW}(0)}{M_W^2} - \frac{\Pi_{ZZ}(-M_Z^2)}{M_Z^2} \right] \quad (4.4)$$

for the various new representations of particles. We will now present a number of such calculations. We will find that new particles in the few hundred GeV mass range give contributions to δA_{LR} which are typically of order 0.01. This is a small correction on an absolute scale but, as we have already noted, quite sizeable compared with the expected accuracy¹ of experiments at the Z^0 . Let us now calculate these contributions for heavy fermions and bosons with definite $SU(2) \times U(1)$ quantum numbers, and also for the pseudo-Goldstone bosons of technicolor models.

Let us first compute the shift δA_{LR} associated with a pair of heavy fermions which couple to the weak interactions as a conventional left-handed doublet. Let the masses of the two members of a weak doublet to be m_T, m_B . If the fermions have color, we must include a factor \mathcal{N}_c for the color multiplicity.

Some typical values of the contribution to the longitudinal polarization asymmetry from quark and lepton doublets are shown in Fig. 10 and 11. Note that, for a doublet with large isospin splitting, δA_{LR} increase proportional to $(m_T^2 - m_B^2)/M_Z^2$. For $m_T \gg M_Z, m_B$, we find:

$$\delta A_{LR} \rightarrow \frac{4 \sin^2 \theta_w}{(1 + v_\theta^2)^2} \frac{\alpha}{\pi} \mathcal{N}_c \left[\frac{m_T^2}{M_Z^2} \right]. \quad (4.5)$$

A similar effect has been noted some time ago in the analogous calculation for the ρ parameter¹³ and has been used there to put a bound of a few hundred GeV on the isospin splittings of quark doublets. Experiments on the polarization asymmetry will clearly place a much stronger bound. A more interesting aspect of our result is that, even in the case of exact isospin degeneracy, a single additional generation of fermions produces an observable effect which is almost independent of mass. For $m_T = m_B \gg M_Z$, one finds that certain of the Δ_i tend to zero:

$$\Delta_\alpha(q^2) \rightarrow 0 \quad (4.6)$$

$$\Delta_\rho(0) \rightarrow 0 \quad (4.7)$$

so that there is decoupling of a heavy degenerate doublet for the ρ parameter or

in the renormalization of α . However, in contrast to the ρ parameter, we find

$$\delta A_{LR} \rightarrow -\frac{8 \sin^2 \theta_w}{(1 + v_\beta^2)^2} \frac{\alpha}{3\pi} \mathcal{N}_c \quad (4.8)$$

$$\simeq \begin{cases} -0.0040 & \text{for one quark doublet} \\ -0.0013 & \text{for one lepton doublet} \end{cases}$$

Numerically, this result is already correct to better than 5% for $m_T = m_B > 100$ GeV. It is a bit surprising at first sight that isospin-degenerate heavy fermions do not decouple. It has been known for some time, though, that heavy fermions need not decouple from low-energy processes in models with axial-current couplings;¹⁹ the contributions of heavy fermions to the axion mass²⁰ and to the mass of the W^\pm ¹⁴ provide other examples of this phenomenon. This result that δA_{LR} is independent of the fermion mass presumably breaks down when the fermions become strongly coupled to the Higgs sector; this requires $m_T \approx 500$ GeV.²¹ Nevertheless, this result, depicted graphically in Fig. 12 shows that, in principle, sufficiently accurate determinations of the longitudinal polarization asymmetries, and to a lesser extent the charge and transverse polarization asymmetries, are capable of “counting” heavy generations of quarks and leptons with non-zero *axial* vector couplings to gauge particles.

The corresponding calculations for a weak doublet of scalars are also quite straightforward. As examples, we display in Figs. 13 and 14 the oblique contributions to δA_{LR} from the scalars which are the supersymmetric partners of, respectively, a quark and a lepton doublet. For simplicity we examine the case in which “left” and “right” squarks (and sleptons) \tilde{q}_L and \tilde{q}_R , the SUSY partners of left and right handed quarks q_L and q_R (and leptons), are good mass eigenstates. The more general case with left-right squark mixing has also been examined^{6,15}

and has been included in the supergravity-motivated SUSY models discussed later. Note that the divergence which we saw above in the case of large isospin splittings for fermions is still present for bosons; for $m_{\tilde{T}} \gg m_{\tilde{B}}, M_Z$ Eq. (4.5) is replaced by:

$$\delta A_{LR} \rightarrow \frac{4 \sin^2 \theta_w}{(1 + v_\phi^2)^2} \frac{\alpha}{\pi} \mathcal{N}_c \left[\frac{m_{\tilde{T}}^2}{M_Z^2} \right]. \quad (4.9)$$

However, the contribution of the bosons to δA_{LR} does tend to zero in the limit of large but isospin-degenerate boson masses. In this case, the Appelquist-Carazone decoupling theorem²² does apply.

These considerations apply only to those bosons which form multiplets under the weak-interaction symmetry. This will not generally be true for bosons which arise from the Higgs sector. In that case, the new bosons will have definite electric charge and perhaps also definite quantum numbers under a custodial isospin symmetry, but they should not have definite $SU(2) \times U(1)$ quantum numbers if they are formed in the symmetry-breaking process. In one class of models, however, a fairly general analysis can still be made: In technicolor models, in which new bosons appear as pseudo-Goldstone bosons associated with the symmetry-breaking, one can use an effective-Lagrangian description of the interactions of these Goldstone bosons to compute their influence on weak-interaction processes.²³ The various vacuum polarization amplitudes depend on the value of an explicit cutoff, Λ_T , which should be taken to be the mass scale of the new hadrons of the technicolor theory. Since the Goldstone bosons are described only by an effective Lagrangian, valid for energies well below Λ_T , it is unreasonable to expect that their contribution will be cutoff-independent and unambiguous. The effective theory of technicolor bosons is not then renormalizable from the point

of view of $SU_2 \times U_1$ (although of course the gauge theory of technifermions is) and this will induce large radiative corrections $\sim \ln(\Lambda_T^2/M_Z^2)$. Further, there are usually a huge number of such Goldstone bosons and their mass matrix breaks global SU_2 quite badly since some are very heavy while others are constrained to be the longitudinal components of the W^\pm and Z^0 . Thus, technicolor (and most composite) models give very large radiative corrections to low energy processes and will affect A_{LR} and M_W dramatically.

The contribution to δA_{LR} from pseudo-Goldstone bosons is easily assembled from (4.4). In Fig. 15, we display this contribution for two typical multiplets, a set of states with the quantum numbers of LQ (and their antiparticles) and a set of color-octet states with the quantum numbers of $\bar{Q}Q$, where, in each case, L and Q represent, respectively, a lepton and a quark doublet. The particles within each multiplet are taken to have almost exactly equal masses; that is the expected situation.²⁴ We note that the corrections are huge for technicolor and should be observable at SLC/LEP.

We next move on to direct corrections from SUSY. As shown in the previous section, these also can be interpreted as effective additions to $\sin^2 \theta_w$ on Z^0 resonance and so Eqs. (4.1) and (4.2) still apply for A_{FB} and A_\perp but we must now use (3.5) (dropping of course the 0.06 in Δ_p since this was included in the GSW prediction) for δA_{LR} . We show in Figs. 16 and 17 the shifts δA_{LR} due to a generic class of SUSY theories (including both oblique and direct-corrections) in which the SUSY breaking scale is motivated by supergravity (SUGRA). These models give mass spectra which depend on the gravitino mass $m_{3/2}$. In particular, as $m_{3/2}$ gets large the squarks in an isospin doublet become degenerate and heavy and thus decouple (as in Figs. 13 and 14) from the rest of the model

at the one-loop level. In some models (the renormalization group or “no-scale” models), a very large top quark mass is used to break the internal symmetry $SU_2 \times U_1 \rightarrow U_1^{\text{QED}}$ after inclusion of radiative corrections and this effect can be seen in the figures. The dependence on the specific Majorana SUSY-breaking “gaugino” masses M_2 (for SU_2) and M_1 (for U_1) is slight.

We now go on to discuss radiative corrections in Bhabha scattering. Unless the new particles are light enough to be produced on Z^0 resonance there will be no interference between the Z^0 and photon exchange diagrams in μ -pair production or Bhabha scattering. Then from (2.4) we can see that on resonance the only new information in Bhabha scattering not suppressed kinematically is in the quantity Δ_α in the t -channel photon exchange for $\cos \theta \gg 0$ with θ the angle between incoming and outgoing electrons. Let us study the response of the ratio X defined in (3.32) to new physics at one loop. Neglecting direct corrections, s -channel photon exchange, t -channel Z^0 exchange and interference terms between s -channel Z^0 and t -channel photon exchange we have on Z^0 resonance

$$\begin{aligned}
X = & (8(1 + \cos \theta)^2 + 32) \left[\frac{\Gamma_Z^0 s_\theta^2 c_\theta^2 (1 - C_\Gamma \Delta_p(-M_Z^2))}{M_Z (1 - \Delta_\alpha(-t))} \right]^2 \\
& \times \left[[(s_\theta^2 + \Delta_p(-M_Z^2))^4 + (-\frac{1}{2} + s_\theta^2 + \Delta_p(-M_Z^2))^4] (1 + \cos \theta)^2 \right. \\
& \left. + 2(s_\theta^2 + \Delta_p(-M_Z^2))^2 (-\frac{1}{2} + s_\theta^2 + \Delta_p(-M_Z^2))^2 (1 - \cos \theta)^2 \right]^{-1}.
\end{aligned} \tag{4.10}$$

Note however that $\Delta_\alpha(\cos \theta = 1) = 0$ so that forward Bhabha scattering again contains information only about $\Delta_p(-M_Z^2)$. Our only hope then is in the *endcap* region $\cos \theta \sim 0.7$ to 0.9 where $\sqrt{-t} \sim 40$ to 20 GeV. We would comment though that for many oblique corrections Δ_α is disappointingly small in this region.

For example in theories with extra quarks and leptons whose mass matrices break badly a global $SU(2)$ isospin symmetry, the μ pair longitudinal polarization asymmetry blows up quadratically with large splitting within the doublet. In Δ_α evaluated in the endcap region such a doublet would decouple completely and there would be no contribution if the lightest member had mass much larger than 40 GeV.

We now discuss the shifts in the precise value of the W^\pm mass due to new physics;^{6,14,15} we have only to examine the quantity

$$\begin{aligned} \delta M_W = \frac{c_\theta M_Z}{2} \left(\frac{-s_\theta^2}{1-2s_\theta^2} \right) \text{Re} \left\{ \frac{\Pi_{WW}(0)}{M_W^2} - \Pi'_{AA}(0) \right. \\ \left. - \frac{c_\theta^2}{s_\theta^2} \frac{\Pi_{ZZ}(-M_Z^2)}{M_Z^2} + \frac{1-s_\theta^2}{s_\theta^2} \frac{\Pi_{WW}(-M_W^2)}{M_W^2} \right. \\ \left. + \Gamma_+^{e\nu_e W}(0) + \Gamma_+^{\mu\nu_\mu W}(0) + V_{++}^{\nu_\mu\mu\nu_e}(0) \right\} \end{aligned} \quad (4.11)$$

for the various new representations of particles where $\Gamma_+^{e\nu_e W}$, $\Gamma_+^{\mu\nu_\mu W}$ and $V_{++}^{\nu_\mu\mu\nu_e}$ came from muon decay (see Figs. 4,5,6,7 and Eqs. (2.17) and (2.24)). Some interesting results are

(1) for an extra doublet with large isospin breaking in the $m_T \gg m_B$ mass matrix

$$\frac{\delta M_W}{M_W} \rightarrow \frac{\alpha}{\pi} \frac{\mathcal{N}_c}{32} \frac{1}{s_\theta^2(1-2s_\theta^2)} \frac{m_T^2}{M_Z^2} \quad (4.12)$$

(2) for an extra quark or lepton doublet with large degenerate mass

$$\delta M_W \rightarrow -\frac{\alpha \mathcal{N}_c}{24\pi(1-2s_\theta^2)} \cdot M_W \simeq - \begin{cases} -14 \text{ MeV} & \text{for leptons} \\ -42 \text{ MeV} & \text{for quarks} \end{cases} \quad (4.13)$$

The shifts δM_W are plotted against those of δA_{LR} for an extra quark and lepton

doublet in Figs. 18 and 19.

(3) the shift due to a squark or slepton doublet with large isospin splitting in the mass matrix is $m_{\tilde{T}} \gg m_{\tilde{B}}$

$$\frac{\delta M_W}{M_W} \rightarrow \frac{\alpha}{\pi} \frac{N_c}{32} \frac{1}{s_\theta^2(1-2s_\theta^2)} \frac{m_{\tilde{T}}^2}{M_Z^2} \quad (4.14)$$

(4) the shift due to a heavy degenerate squark or slepton doublet is

$$\delta M_W \rightarrow 0 \quad (4.15)$$

(5) Technicolor models can change the value of the W^\pm mass considerably. The shift δM_W is plotted against δA_{LR} in Fig. 20.

(6) We give the complete shifts δM_W from two classes of SUGRA models including all oblique and direct couplings; boxes, vertices and fermion and vector boson self-energies in Figs. 21 and 22. These are from the work of Lynn¹⁵ and Lynn and Peskin.⁶

Finally, we would like to add a comment on anomalous vacuum expectation values (v.e.v.'s). All of the previous work in this paper was based on the assumption that the symmetry breaking $SU_1 \times U_1 \rightarrow U_1^{\text{QED}}$ was done by Higgs' doublets. Let us imagine that some representation of scalars which is *not* a doublet (say, a Higgs' triplet) acquired a small v.e.v.: There would be two effects of such a representation on various experimentally measurable quantities;

- a) the new representation of scalars would enter into one-loop diagrams such as in Figs. 3,4,5,6,7 and contribute to radiative corrections as previously discussed.

b) The Higgs' v.e.v.'s would affect tree level formulae. We will now discuss this latter contribution. The $W^\pm - Z^0$ mass relation would be changed to

$$\frac{M_W^2}{M_Z^2} = \rho \frac{g^2}{g^2 + g'^2}$$

$$\rho = 1 + \delta\rho \tag{4.16}$$

$$\delta\rho = \frac{2 \sum_{\text{scalars}} \lambda_i^2 (I_i^2 + I_i - \frac{3}{4} Y_i^2)}{\sum_{\text{scalars}} \lambda_i^2 Y_i^2}$$

where λ_i, I_i, Y_i are the v.e.v., weak isospin and hypercharge of the i^{th} scalar representation; for neutral particles $I_{3i} = -\frac{Y_i}{2}$. If we assume $\delta\rho \ll 1$ and throw away terms $\mathcal{O}(\delta\rho)^2$ and $\mathcal{O}(\alpha\delta\rho)$ in keeping with the experimental value $\rho \simeq 1$, the formulae (2.4) and (2.20) will still be correct provided we make the displacements.²⁵

$$\Delta_\rho \rightarrow \Delta_\rho + \delta\rho$$

$$\Delta_p \rightarrow \Delta_p - \frac{s_\theta^2 c_\theta^2}{1 - 2s_\theta^2} \delta\rho$$

$$\Delta_\alpha \rightarrow \Delta_\alpha$$

$$\Delta_W \rightarrow \Delta_W + \frac{c_\theta^2}{1 - 2s_\theta^2} \delta\rho .$$
(4.17)

This would cause the shifts in the physical quantities listed in Table IX. These have been evaluated for $M_Z = 94$ GeV and $\delta\rho = 0.01$ in order to see the generic magnitude of the effect. Note that, contrary to popular belief, $R_{NC;CC}$ is not the best place to look for the effects of anomalous v.e.v.'s; M_W and A_{LR} are.

5. Conclusions

Radiative corrections can affect the values of the various asymmetries in $e^+e^- \rightarrow \mu^+\mu^-, \tau^+\tau^-$ as well as the W^\pm mass in measurable ways. Our most important conclusion is that all radiative corrections to four-lepton processes can be reduced to a few functions. The fact that precision probes of the weak interactions involve only a few specific quantities is a great aid in evaluating and comparing experiments on weak radiative corrections. Especially exciting is the possibility of seeing the effects of new particles from beyond the standard model, even if they are too heavy to be produced directly at LEP/SLC, via radiative corrections. We present a summary list of generic values of shifts to various physical quantities due to radiative corrections from various sources in Table X. Also present there is an estimate of the theoretical uncertainty⁷ due to strong interactions and light hadrons from the QED vacuum polarization diagrams of Fig. 1 entering as in Eq. (1.7). Lepton asymmetries on Z^0 resonance are more sensitive to the effects of radiative corrections with the observation of longitudinal polarization than without.

REFERENCES

1. A good review of LEP/SLC and HERA and Tevatron physics is given in the Proceedings of the Conference on "Tests of Electroweak Theories", Trieste, Italy, June, 1985, B. W. Lynn and C Verzeqnessi editors, World Scientific Pubs, Singapore (1985); SLC Workshop, SLAC Report 247 (1982); Cornell Z^0 Theory Workshop, February, 1981, M. E. Peskin and S.-H. H. Tye, editors; 1978 LEP study group CERN 79-01 (1979).
2. G. Bardin *et. al.*, Phys. Letts. 137B (1984) 135.
3. A. Sirlin, Phys. Rev. D22 (1980) 285; A. Sirlin in Proceedings of the 1983 Trieste Workshop on Radiative Corrections in $SU_2 \times U_1$, B. W. Lynn and J. F. Wheeler, editors, World Scientific Pubs, Singapore (1984).
4. W. J. Marciano in Cornell Workshop, Ref. 1; *ibid*, Ref. 8.
5. B. W. Lynn and R. G. Stuart, Nucl. Phys. B253 (1985) 216; R. G. Stuart, Oxford University, D. Phil Thesis (1985).
6. B. W. Lynn and M. E. Peskin, SLAC-PUB-3724 (1985).
7. J. Cole *et. al.*, ISAS preprint 19/85/EP, Trieste, Italy; B. W. Lynn, G. Penso and C. Verzeqnessi, SLAC-PUB-3742 (1985).
8. W. J. Marciano and A. Sirlin, Nucl. Phys. B189 (1981) 442; W. J. Marciano, Phys. Rev. D20 (1979) 274; A. Sirlin, Phys. Rev. D29 (1984) 89.
9. F. A. Berends and R. Kleiss, Nucl. Phys. B117 (1981) 237; F. A. Berends, R. Kleiss and S. Jadach, Nucl. Phys. B202 (1982) 63; *ibid*. Comp. Phys. Comm. 29 (1983) 29; M. Greco *et. al.*, Nucl. Phys. B17 (1980) 181,

- errata Nucl. Phys. B197 (1981) 543; QED radiative corrections to polarized $e^+e^- \rightarrow f\bar{f}(\gamma)$ were first calculated by M. Bohm and W. Hollik, Nucl. Phys. B204 (1982) 45; Monte Carlo event generating computer programs for $e^+e^- \rightarrow \mu^+\mu^-(\gamma)$ including all GSW corrections are available at CERN/SLAC, R. Kleiss, B. W. Lynn and R. G. Stuart (1985).
10. C. Busi *et. al.*, CHARM II collaboration, CERN/SPSC/83-87 (1983).
 11. B. W. Lynn and R. G. Stuart, SLAC-PUB-3738 (1985).
 12. M. Hayashi and K. Katsurra, Nuovo Cimento Lett. 39 (1984) 171.
 13. E. Eliasson, Northeastern University preprint NUB-2621 (1983); R. Barbieri and L. Maiani, Nucl. Phys. B224 (1983) 32; C. S. Lim *et. al.*, Phys. Rev. D29 (1984) 1488; R. Renken and M. E. Peskin, Cornell University preprint CLNS 82/540 (1982); M. B. Einhorn *et. al.*, Nucl. Phys. B191 (1981) 146; M. Veltman, Nucl. Phys. B231 (1984) 205; A. Cohen *et. al.*, Nucl. Phys. B232 (1984) 61.
 14. W. J. Marciano and A. Sirlin, Brookhaven preprint BNL 33819; S. Bertolini and A. Sirlin, NYU preprint NYU-TR3-84 (1984); J. A. Grifols and J. Sola, Phys. Letts. 137B (1984) 257; A. Sirlin, Phys. Rev. D22 (1980) 971; M. Consoli *et. al.*, Nucl. Phys. B223 (1983) 474; see also the Proceedings of Ref. 3.
 15. B. W. Lynn, SLAC-PUB-3358 (1984).
 16. G. Passarino and M. Veltman, Nucl. Phys. B160 (1979) 151; R. W. Brown *et. al.*, Phys. Rev. Lett. 52 (1984) 1192; J. P. Cole in Proceedings of Ref. 3; W. Wetzel, Nucl. Phys. B227 (1983) 1; R. J. Cashmore *et. al.*, Oxford Nucl. Phys. Preprint 45/85; S. Bellucci, Nuovo Cimento 80A (1984) 279; W. Hollik, DESY preprint 84075 (1984).

17. M. Bohm *et. al.*, DESY preprint 84-040 (1984); M. Consoli, Nucl. Phys. B160 (1979) 208.
18. S. Sarantakos and A. Sirlin, Nucl. Phys. B217 (1983) 84; M. Bohm *et. al.*, DESY preprint DESY-84-067 (1984); D. Yu. Bardin, Nucl. Phys. B246 (1984) 221; K. I. Aoki *et. al.*, Prog. Theor. Phys. 65 (1981) 1001; W. J. Marciano and A. Sirlin, Phys. Rev. D22 (1980) 2695.
19. J. Collins, F. Wilczek, and A. Zee, Phys. Rev. D18 (1978) 242.
20. M. E. Peskin (unpublished)
21. M. S. Chanowitz *et. al.*, Nucl. Phys. B153 (1979) 402; *ibid*, Phys. Letts. 76B (1978) 285.
22. T. Applequist and J. Carrazone, Phys. Rev. D11 (1975) 2856.
23. S. Chadha and M. E. Peskin, Nucl. Phys. B185 (1981) 61; *ibid*. Nucl. Phys. B187 (1981) 541.
24. M. E. Peskin, Nucl. Phys. B175 (1980) 197; J. P. Preskill, Nucl. Phys. B177 (1981) 21.
25. I. Leide, B. W. Lynn and S. Sakakibara (unpublished).

TABLE CAPTIONS

- I.* Initial state longitudinal polarization asymmetry A_{LR} on Z^0 resonance in $e^+e^- \rightarrow \mu^+\mu^-$ for various M_Z, m_H, m_t to one-loop in GSW. All masses are in GeV.
- II.* Forward-backward or charge asymmetry A_{FB} on Z^0 resonance in $e^+e^- \rightarrow \mu^+\mu^-$ for various M_Z, m_H, m_t to one-loop in GSW. All masses are in GeV.
- III.* Transverse polarization asymmetry A_{\perp} on Z^0 resonance for $e^+e^- \rightarrow \mu^+\mu^-$ for various M_Z, m_H, m_t to one-loop in GSW. All masses are in GeV.
- IV.* The ratio of Bhabha scattering to μ pair production on Z^0 resonance
- $$X = \left[\frac{\frac{d\sigma}{dt}(e^+e^- \rightarrow e^+e^-)}{\frac{d\sigma}{dt}(e^+e^- \rightarrow \mu^+\mu^-)} - 1 \right]_{s=M_Z^2} (1 - \cos \theta)^2$$
- for various $\cos \theta, M_Z, m_H, m_t$ to one-loop in GSW. All masses are in GeV.
- V.* The Z^0 decay width Γ_Z to one-loop in GSW for various M_Z, m_t, m_H . Fermion masses have been neglected in 1PI vertex and fermion self energy parts but included in 1PI vector boson self-energies. Strong interactions have been neglected. All masses are in GeV.
- VI.* The W^{\pm} mass M_W to one-loop in GSW for various M_Z, m_t, m_H . All masses are in GeV.
- VII.* $R_{\nu\bar{\nu}}$ ratio of neutral current muon neutrino to muon antineutrino-electron scattering to leptons for incoming neutrino energy $E_{\nu} = 70$ in electron rest frame for various M_Z, m_H, m_t . All masses are in GeV.
- VIII.* $R_{NC;CC}$ ratio of neutral to charged current muon neutrino electron scattering to leptons for incoming neutrino energy $E_{\nu} = 70$ in electron rest frame for various M_Z, m_H, m_t . All masses are in GeV.

- IX.* Shifts of various quantities due to v.e.v.'s of scalars *not* in doublet representations.
- X.* Responses at one-loop of various asymmetries on Z^0 resonance and the W^\pm mass to new one-loop physics. Numbers are generic, calculated using $M_Z = 94$ GeV.

Table I

Initial state longitudinal polarization asymmetry A_{LR} on Z^0 resonance in
 $e^+e^- \rightarrow \mu^+\mu^-$ for various M_Z, m_H, m_t to
 one-loop in GSW. All masses are in GeV.

$$A_{LR}(q^2 = -M_Z^2)$$

	M_Z	$m_H = 10$	$m_H = 100$	$m_H = 1000$
$m_t = 30$	90	.0613	.0536	.0423
	92	.1762	.1691	.1590
	94	.2756	.2692	.2602
	96	.3615	.3557	.3475
	98	.4354	.4302	.4229
$m_t = 60$	90	.0640	.0563	.0451
	92	.1786	.1716	.1615
	94	.2777	.2714	.2624
	96	.3633	.3575	.3495
	98	.4370	.4318	.4246
$m_t = 90$	90	.0703	.0626	.0513
	92	.1844	.1773	.1672
	94	.2830	.2767	.2676
	96	.3681	.3624	.3543
	98	.4414	.4362	.4290
$m_t = 130$	90	.0805	.0728	.0616
	92	.1936	.1866	.1765
	94	.2914	.2851	.2760
	96	.3757	.3699	.3619
	98	.4482	.4430	.4358
$m_t = 180$	90	.0975	.0898	.0786
	92	.2087	.2018	.1918
	94	.3048	.2986	.2897
	96	.3876	.3819	.3741
	98	.4589	.4537	.4467

Table II

Forward-backward or charge asymmetry A_{FB}
on Z^0 resonance in $e^+e^- \rightarrow \mu^+\mu^-$ for various M_Z ,
 m_H, m_t to one-loop in GSW. All masses are in GeV.

$$A_{FB}(q^2 = -M_Z^2)$$

	M_Z	$m_H = 10$	$m_H = 100$	$m_H = 1000$
$m_t = 30$	90	.0046	.0039	.0028
	92	.0255	.0236	.0209
	94	.0596	.0570	.0532
	96	.1011	.0979	.0934
	98	.1457	.1422	.1374
$m_t = 60$	90	.0044	.0037	.0025
	92	.0256	.0237	.0208
	94	.0599	.0572	.0533
	96	.1014	.0982	.0936
	98	.1460	.1425	.1375
$m_t = 90$	90	.0047	.0041	.0033
	92	.0269	.0251	.0226
	94	.0619	.0593	.0558
	96	.1039	.1008	.0965
	98	.1487	.1454	.1407
$m_t = 130$	90	.0046	.0040	.0036
	92	.0282	.0265	.0245
	94	.0643	.0618	.0587
	96	.1069	.1039	.1001
	98	.1522	.1489	.1447
$m_t = 180$	90	.0032	.0028	.0030
	92	.0292	.0276	.0263
	94	.0668	.0645	.0620
	96	.1105	.1077	.1045
	98	.1564	.1533	.1498

Table III

Transverse polarization asymmetry A_{\perp} on Z^0 resonance for $e^+e^- \rightarrow \mu^+\mu^-$ for various M_Z , m_H , m_t to one-loop in GSW. All masses are in GeV.

$$A_{\perp} (q^2 = -M_Z^2)$$

	M_Z	$m_H = 100$	$m_H = 1000$
$m_t = 30$	90	-0.9865	-0.9871
	94	-0.9507	-0.9533
	98	-0.8904	-0.8939
$m_t = 180$	90	-0.9883	-0.9881
	94	-0.9471	-0.9486
	98	-0.8844	-0.8866

Table IV

The ratio of Bhabha scattering to μ pair production on Z^0 resonance

for various $\cos \theta$, M_Z , m_t , m_H to one loop in GSW. All masses

$$\text{are in GeV. } X = \left[\frac{\sigma(e^+e^- \rightarrow e^+e^-)}{\sigma(e^+e^- \rightarrow \mu^+\mu^-)} - 1 \right]_{s=M_Z^2} (1 - \cos \theta)^2$$

$m_t = 30, m_H = 100$				$m_t = 180, m_H = 100$			
$\cos \theta$	$M_Z = 90$	$M_Z = 94$	$M_Z = 98$	$\cos \theta$	$M_Z = 90$	$M_Z = 94$	$M_Z = 98$
1.0000	0.0510	0.0498	0.0454	1.00	0.0436	0.0405	0.0356
0.99	0.0532	0.0519	0.0474	0.99	0.0454	0.0422	0.0371
0.90	0.0543	0.0532	0.0487	0.90	0.0465	0.0433	0.0383
0.80	0.0547	0.0537	0.0494	0.80	0.0468	0.0438	0.0389
0.70	0.0547	0.0540	0.0500	0.70	0.0469	0.0441	0.0394
0.60	0.0545	0.0541	0.0505	0.60	0.0468	0.0443	0.0399
0.50	0.0541	0.0540	0.0509	0.50	0.0464	0.0443	0.0403
0.40	0.0533	0.0536	0.0511	0.40	0.0459	0.0441	0.0406
0.30	0.0522	0.0529	0.0511	0.30	0.0448	0.0436	0.0407
0.20	0.0506	0.0519	0.0509	0.20	0.0434	0.0428	0.0407
0.10	0.0486	0.0504	0.0504	0.10	0.0417	0.0416	0.0403
0.0	0.0463	0.0485	0.0492	0.0	0.0397	0.0401	0.0396
-0.10	0.0435	0.0461	0.0477	-0.10	0.0372	0.0381	0.0384
-0.20	0.0406	0.0434	0.0460	-0.20	0.0347	0.0360	0.0377
-0.30	0.0376	0.0405	0.0436	-0.30	0.0321	0.0336	0.0351
-0.40	0.0346	0.0375	0.0410	-0.40	0.0295	0.0310	0.0329
-0.50	0.0317	0.0345	0.0381	-0.50	0.0269	0.0285	0.0306
-0.60	0.0289	0.0315	0.0351	-0.60	0.0245	0.0261	0.0282
-0.70	0.0263	0.0287	0.0322	-0.70	0.0223	0.0237	0.0259
-0.80	0.0238	0.0260	0.0293	-0.80	0.0202	0.0215	0.0236
-0.90	0.0215	0.0235	0.0265	-0.90	0.0182	0.0194	0.0213
-0.99	0.0195	0.0214	0.0240	-0.99	0.0166	0.0176	0.0194
-1.00	0.0193	0.0211	0.0238	-1.00	0.0164	0.0175	0.0191

$m_t = 30, m_H = 1000$				$m_t = 180, m_H = 1000$			
$\cos \theta$	$M_Z = 90$	$M_Z = 94$	$M_Z = 98$	$\cos \theta$	$M_Z = 90$	$M_Z = 94$	$M_Z = 98$
1.00	0.0516	0.0507	0.0464	1.00	0.0441	0.0413	0.0365
0.99	0.0537	0.0528	0.0484	0.99	0.0460	0.0431	0.0381
0.90	0.0549	0.0541	0.0498	0.90	0.0470	0.0442	0.0392
0.80	0.0552	0.0546	0.0505	0.80	0.0473	0.0447	0.0399
0.70	0.0552	0.0549	0.0510	0.70	0.0474	0.0450	0.0404
0.60	0.0550	0.0550	0.0515	0.60	0.0473	0.0451	0.0408
0.50	0.0546	0.0548	0.0518	0.50	0.0469	0.0451	0.0412
0.40	0.0538	0.0544	0.0520	0.40	0.0463	0.0449	0.0415
0.30	0.0526	0.0537	0.0520	0.30	0.0453	0.0444	0.0416
0.20	0.0510	0.0526	0.0517	0.20	0.0439	0.0435	0.0415
0.10	0.0490	0.0510	0.0511	0.10	0.0422	0.0423	0.0411
0.0	0.0466	0.0490	0.0501	0.0	0.0403	0.0407	0.0402
-0.10	0.0439	0.0465	0.0490	-0.10	0.0377	0.0387	0.0389
-0.20	0.0409	0.0438	0.0463	-0.20	0.0350	0.0363	0.0373
-0.30	0.0379	0.0409	0.0441	-0.30	0.0327	0.0340	0.0357
-0.40	0.0349	0.0378	0.0414	-0.40	0.0298	0.0315	0.0335
-0.50	0.0319	0.0348	0.0384	-0.50	0.0273	0.0293	0.0311
-0.60	0.0291	0.0318	0.0354	-0.60	0.0248	0.0264	0.0287
-0.70	0.0265	0.0289	0.0324	-0.70	0.0226	0.0243	0.0263
-0.80	0.0240	0.0262	0.0295	-0.80	0.0204	0.0218	0.0239
-0.90	0.0217	0.0237	0.0267	-0.90	0.0185	0.0197	0.0217
-0.99	0.0197	0.0215	0.0242	-0.99	0.0168	0.0179	0.0197
-1.00	0.0195	0.0213	0.0240	-1.00	0.0166	0.0177	0.0194

Table V

The Z^0 decay width Γ_Z to one-loop in GSW for various M_Z , m_t , m_H . Fermion masses have been neglected in 1PI vertex and fermion self energy parts but included in 1PI vector boson self-energies. Strong interactions have been neglected. All masses are in GeV.

Γ_Z			
	M_Z	$m_H = 100$	$m_H = 1000$
$m_t = 30$	90	2.4631	2.4532
	94	2.8991	2.8853
	98	3.3866	3.3684
$m_t = 180$	90	2.3694	2.3616
	94	2.7786	2.7681
	98	3.2344	3.2213

Table VI

The W^\pm mass M_W to one-loop in GSW for various M_Z , m_t , m_H . All masses are in GeV.

		M_W			
		M_Z	$m_H = 10$	$m_H = 100$	$m_H = 1000$
$m_t = 30$	90	78.37	78.29	78.12	
	92	80.88	80.80	80.64	
	94	83.33	83.26	83.10	
	96	85.74	85.66	85.51	
	98	88.11	88.03	87.88	
$m_t = 60$	90	78.36	78.27	78.11	
	92	80.86	80.78	80.62	
	94	83.30	83.22	83.06	
	96	85.69	85.62	85.46	
	98	88.05	87.98	87.82	
$m_t = 90$	90	78.55	78.47	78.30	
	92	81.06	80.98	80.81	
	94	83.50	83.43	83.27	
	96	85.90	85.82	85.67	
	98	88.26	88.18	88.03	
$m_t = 130$	90	78.79	78.70	78.53	
	92	81.30	81.22	81.05	
	94	83.75	83.67	83.51	
	96	86.16	86.08	85.92	
	98	88.53	88.45	88.29	
$m_t = 180$	90	79.14	79.06	78.88	
	92	81.66	81.57	81.40	
	94	84.12	84.04	83.87	
	96	86.54	86.46	86.29	
	98	88.92	88.84	88.67	

Table VII

$R_{\nu\bar{\nu}}$ ratio of neutral current muon neutrino to muon antineutrino-electron scattering to leptons for incoming neutrino energy $E_\nu = 70$ in electron rest frame to one-loop in GSW for various M_Z , m_H , m_t . All masses are in GeV.

$$R_{\nu\bar{\nu}} = \frac{\sigma(\nu_\mu e \rightarrow \nu_\mu e)}{\sigma(\bar{\nu}_\mu e \rightarrow \bar{\nu}_\mu e)}$$

	M_Z	$m_H = 100$	$m_H = 1000$
$m_t = 30$	90	1.0325	1.0065
	94	1.2862	1.2572
	98	1.5224	1.4920
$m_t = 180$	90	1.1598	1.1297
	94	1.4352	1.4022
	98	1.6841	1.6504

Table VIII

$R_{NC,CC}$ ratio of neutral to charged current muon neutrino electron scattering to leptons for incoming neutrino energy $E_\nu = 70$ in electron rest frame to one-loop in GSW for various M_Z , m_H , m_t . All masses are in GeV.

$$R_{NC,CC} = \frac{\sigma(\nu_\mu e \rightarrow \nu_\mu e)}{\sigma(\nu_\mu e \rightarrow \nu_e \mu)}$$

	M_Z	$m_H = 100$	$m_H = 1000$
$m_t = 30$	90	0.1158	0.1145
	94	0.1295	0.1281
	98	0.1424	0.1409
$m_t = 180$	90	0.1204	0.1193
	94	0.1344	0.1333
	98	0.1471	0.1462

Table IX

Shifts in various quantities due to v.e.v.'s of
scalars *not* in doublet representations

Shift	Formula for Shift	Shift Evaluated $M_Z = 94 \text{ GeV}, \delta\rho = .01$	Comments
$\delta A_{LR} = \delta A_{\tau pol}$	$\frac{64s_\theta^4 c_\theta^2}{(1+v_\theta^2)^2} \delta\rho$.021	initial or final state longitudinal polarization asymmetry $e^+e^- \rightarrow \mu^+\mu^-, \tau^+\tau^-$ on Z^0 resonance
δA_{FB}	$-\frac{192v_\theta s_\theta^4 c_\theta^2}{(1+v_\theta^2)^3} \delta\rho$.0094	charge asymmetry $e^+e^- \rightarrow \mu^+\mu^-$ on Z^0 resonance
δA_\perp	$-\frac{16v_\theta s_\theta^2 c_\theta^2}{(1+v_\theta^2)^2(1-2s_\theta^2)} \delta\rho$.0066	transverse polarization asymmetry $e^+e^- \rightarrow \mu^+\mu^-$ on Z^0 resonance
δM_W	$\frac{c_\theta^2}{2(1-2s_\theta^2)} M_W \delta\rho$	570 MeV	W^\pm mass
$\frac{\delta X(\cos\theta=1)}{X(\cos\theta=1)}$	$\left[\frac{C_\Gamma}{2} + \frac{(s_\theta^2)^3 + (-\frac{1}{2} + s_\theta^2)^3}{(s_\theta^2)^4 + (-\frac{1}{2} + s_\theta^2)^4} \right] \frac{4s_\theta^2 c_\theta^2}{1-2s_\theta^2} \delta\rho$	-.013	ratio Bhabha to $e^+e^- \rightarrow \mu^+\mu^-$ on Z^0 resonance Eq. (4.10) at $\cos\theta = 1$
$\delta\Gamma_Z$	$\left[\frac{C_\Gamma s_\theta^2 c_\theta^2}{1-2s_\theta^2} + 1 \right] \Gamma_Z \delta\rho$	38 MeV	Z^0 width
$\delta\Gamma_W$	$\frac{3}{2} \frac{c_\theta^2}{1-2s_\theta^2} \Gamma_W \delta\rho$	53 MeV	W^\pm width
$\delta R_{\nu\nu}$	$\frac{64s_\theta^4 c_\theta^2}{(1+v_\theta+v_\theta^2)^2} R_{\nu\nu} \delta\rho$.033	ratio of neutral $\nu_\mu e$ to $\bar{\nu}_\mu e$ scattering $E_\nu = 70 \text{ GeV}$
$\delta R_{NC,CC}$	$\left[2 + \frac{4(1-2v_\theta)s_\theta^2 c_\theta^2}{(1-v_\theta+v_\theta^2)(1-2s_\theta^2)} \right] R_{NC,CC} \delta\rho$.0043	ratio of neutral to charge $\nu_\mu e$ scattering $E_\nu = 70 \text{ GeV}$

Table X

Responses at one loop of various asymmetries on Z^0 resonance and the W^\pm mass to new one-loop physics. Numbers are generic, calculated using $M_Z = 94$ GeV

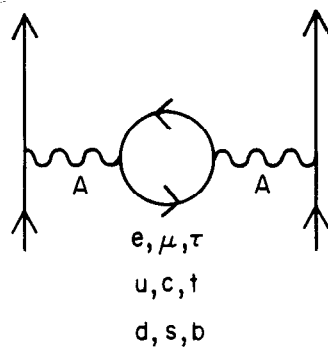
One-Loop Physics	$\delta A_{LR} = \delta A_{rpol}$	δA_{FB}	δA_\perp	δM_W (MeV)
GSW Weak $m_t = 30$ $m_H = 100$	-0.03	-0.01	.005	-180
Heavy Top Quark $m_t \simeq 180$ GeV	0.03	0.0075	0.004	780
Heavy Higgs ~ 1 TeV	-0.01	-0.0045	-0.003	-160
Heavy Quark Pair a) Large I Splitting b) Degenerate	0.02 -0.004	0.01 -0.002	0.007 -0.001	300 -42
Heavy Lepton Pair a) Large I Splitting $m_\nu = 0$ b) Degenerate	0.012 -0.0013	0.006 -0.0006	0.004 -0.0004	300 -14
Heavy Squark Pair a) Large I Splitting b) Degenerate	0.02 0	0.01 0	0.007 0	300 0
Heavy Slepton Pair a) Large I Splitting b) Degenerate	0.012 0	0.006 0	0.004 0	300 0
Winos a) $m_{3/2} \ll 100$ GeV b) $m_{3/2} \gg 100$ GeV	0.005 <0.001	0.0025 <0.001	0.001 $\ll 0.001$	100 <10
Technicolor $SU_8 \times SU_8$ O_{16}	-0.04 -0.07	-0.018 -0.032	-0.012 -0.021	-500 -500
Strong Interaction Uncertainty	± 0.0033	± 0.0016	± 0.001	± 25 MeV

FIGURE CAPTIONS

1. QED vacuum polarization graphs.
2. QED detector dependent graphs specifically *excluded* from 4-fermion processes considered in this paper. To thee we must add all permutations of the photon lines. See Ref. 9.
3. Unrenormalized 1PI vector boson self-energy. i, j refer to the particles Z, A (photon), W^\pm or to the SU_2 isospin 1, 2, 3 and electromagnetic Q currents. Solid lines with arrows are fermions, dashed lines scalars, wavy lines vector particles, and dotted lines with arrows are ghosts.
4. Unrenormalized 1PI fermion self energy.
5. Unrenormalized 1PI fermion Z^0 vertex part.
6. Unrenormalized 1PI fermion W^\pm vertex part. Graphs are similar to those in Fig. 5.
7. 1PI box diagrams contributing to muon decay and the form factor $V_{++}^{\nu_\mu\mu\nu_e}$.
8. Forward-backward asymmetry A_{FB} as a function of \sqrt{s} . The dashed lines include no radiative corrections, not even from QED diagrams of Fig. 1, and the solid lines include all one-loop GSW corrections except those of Fig. 2 for $m_t = 30$ and $m_H = 100$. All masses are in GeV.
9. Longitudinal polarization asymmetry $A_{LR} = A_{\tau_{\text{pol}}}$ as a function of \sqrt{s} . The dashed lines and solid lines are as in Fig. 7. The dotted lines include only the QED graphs of Fig. 1 contribution to the renormalization of α .
10. Contribution of an extra quark doublet to δA_{LR} for various isospin splitting ratios m_B/m_T as a function of m_T . All masses are in GeV.

11. Contributions of an extra lepton doublet to δA_{LR} for various isospin splitting ratios m_ν/m_{ℓ^-} as a function of m_{ℓ^-} . All masses are in GeV.
12. Contributions of heavy degenerate generations of quarks and leptons to δA_{LR} as a function of the fermion mass. All masses are in GeV.
13. Contribution of a squark doublet to δA_{LR} for various isospin splitting ratios $m_{\tilde{B}}/m_{\tilde{T}}$ as a function of $m_{\tilde{T}}$. We ignore mixing between “left” and “right” squarks and take their masses degenerate. All masses in GeV.
14. Contribution of a slepton doublet to δA_{LR} for various isospin splitting ratios $m_{\tilde{\nu}}/m_{\tilde{\ell}^-}$ as a function of $m_{\tilde{\ell}^-}$. We ignore mixings between “left” and “right” sleptons and take their masses degenerate. All masses are in GeV.
15. Contributions of various technicolor models to δA_{LR} as a function of a mass scale which occurs in such models. The contribution from a GSW Higgs is displayed for reference relative to a “standard” value $m_H = 100$. All masses are in GeV.
16. SUSY shifts δA_{LR} in models in which the gaugino masses are related to the SUSY breaking gravitino mass $m_{3/2}$ from SUGRA. All masses are in GeV.
17. SUSY shifts δA_{LR} in models in which the gaugino masses are independent of $m_{3/2}$. In some models they are due to radiative corrections and are small. All masses are in GeV.
18. Shift δM_W versus shift δA_{LR} for an extra quark doublet as a function of m_T . We include the shift due to heavy GSW Higgs’ for reference. All masses are in GeV.

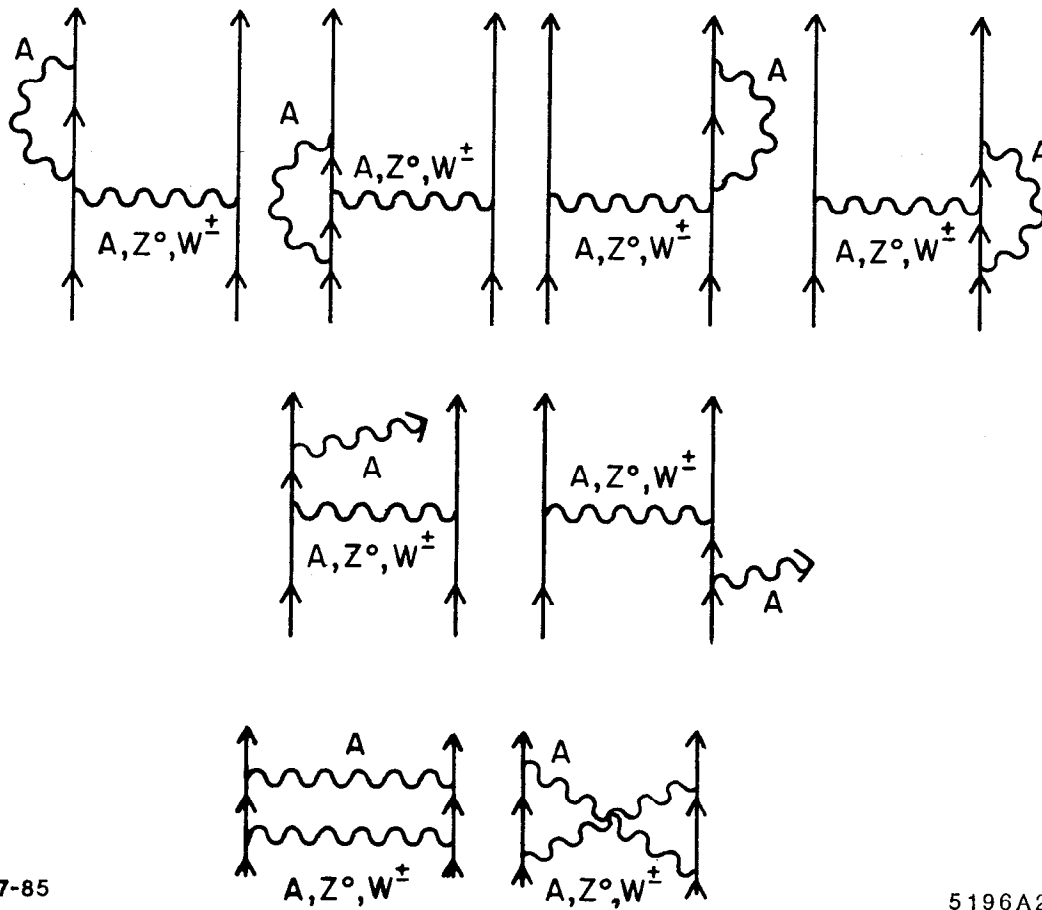
19. Shift δM_W versus shift δA_L for an extra lepton doublet as a function of m_{ℓ^-} . We include the shift due to the GSW Higgs' for reference relative to a "standard" value $m_H = 100$. All masses are in GeV.
20. Shift δM_W versus δA_{LR} for two technicolor models as a function of a scale which enters into such models. We plot also the shift due to the GSW Higgs' for reference relative to a "standard" value $m_H = 100$. All masses are in GeV.
21. SUSY shifts δM_W in models in which the gaugino masses are related to the SUSY breaking gravitino mass $m_{3/2}$ from SUGRA. All masses are in GeV.
22. SUSY shifts δM_W in models in which the gaugino masses are independent of $m_{3/2}$. In some models they are due to radiative corrections and are small. All masses are in GeV.



7-85

5196A1

Fig. 1



7-85

5196A2

Fig. 2

$$\begin{aligned}
 & \xrightarrow{q} \quad \begin{array}{c} \mu \\ \text{---} \text{---} \text{---} \\ i \end{array} \text{---} \text{---} \text{---} \begin{array}{c} \nu \\ \text{---} \text{---} \text{---} \\ j \end{array} = \delta_{\mu\nu} \Pi_{ij} - q_\mu q_\nu \Pi'_{ij} \\
 & = \sum_{\text{fermions}} \text{---} \text{---} \text{---} + \sum_{\substack{\text{vectors} \\ \text{scalars}}} \text{---} \text{---} \text{---} \\
 & + \sum_{\text{vectors}} \text{---} \text{---} \text{---} + \sum_{\text{vectors}} \text{---} \text{---} \text{---} \\
 & + \sum_{\text{scalars}} \text{---} \text{---} \text{---} + \sum_{\text{scalars}} \text{---} \text{---} \text{---} \\
 & + \sum_{\text{ghosts}} \text{---} \text{---} \text{---}
 \end{aligned}$$

8-85
5196A3

Fig. 3

$$\begin{aligned}
& \begin{array}{c} p \\ \longrightarrow \end{array} \begin{array}{c} \text{shaded circle} \\ \longrightarrow \end{array} = i\boldsymbol{\gamma} \cdot \mathbf{A} + mC \\
& = \sum_{\substack{\text{fermions} \\ \text{scalars}}} \begin{array}{c} \text{fermion line} \\ \text{with dashed loop} \\ \longrightarrow \end{array} + \sum_{\substack{\text{fermions} \\ \text{vectors} \neq A}} \begin{array}{c} \text{fermion line} \\ \text{with wavy loop} \\ \longrightarrow \end{array}
\end{aligned}$$

8-85 5196A4

Fig. 4

$$\begin{aligned}
& \text{Diagram: } e \rightarrow \text{blob} \rightarrow e \text{ with } Z \text{ emission} \\
& = ie \frac{I_L^3 - Q s_\theta^2}{s_\theta c_\theta} \gamma_\lambda \gamma_+ \tilde{\Gamma}_+^{eeZ} \\
& \quad + ie \frac{I_R^3 - Q s_\theta^2}{s_\theta c_\theta} \gamma_\lambda \gamma_- \tilde{\Gamma}_-^{eeZ} \\
& = \sum_{\text{vectors fermion}} \text{Diagram 1} + \sum_{\text{vectors} \neq A \text{ fermion}} \text{Diagram 2} \\
& \quad + \sum_{\text{vectors scalars fermion}} \text{Diagram 3} + \sum_{\text{vectors scalars fermion}} \text{Diagram 4} \\
& \quad + \sum_{\text{scalars fermion}} \text{Diagram 5}
\end{aligned}$$

8-85 5196A5

Fig. 5

The diagram shows an incoming electron line (labeled 'e') entering a shaded circular vertex from the left. From this vertex, an outgoing neutrino line (labeled 'ν_e') exits to the right, and a wavy line representing a W boson (labeled 'W') exits downwards.

$$= \frac{ie}{\sqrt{2} s_\theta} \gamma_\lambda \gamma_+ \tilde{\Gamma}_+^{e\nu_e W}$$

7-85 5196A6

Fig. 6

$$\begin{array}{c} \uparrow \nu_\mu \\ \uparrow e \\ \text{---} \\ \uparrow \mu \\ \uparrow \nu_e \end{array} = \frac{-4G_\mu}{\sqrt{2}} (\bar{\nu}_\mu \gamma_\lambda \gamma_+ \mu) (\bar{e} \gamma_\lambda \gamma_+ \nu_e) V_{++}^{\nu_\mu \mu e \nu_e}$$

$$= \sum_{\substack{\text{vector} \neq A \\ \text{fermions}}} \left[\begin{array}{c} \uparrow \\ \uparrow \\ \uparrow \end{array} \begin{array}{c} \uparrow \\ \uparrow \\ \uparrow \end{array} \right] + \left[\begin{array}{c} \uparrow \\ \uparrow \\ \uparrow \end{array} \begin{array}{c} \uparrow \\ \uparrow \\ \uparrow \end{array} \right]$$

$$+ \sum_{\substack{\text{scalars} \\ \text{fermions}}} \left[\begin{array}{c} \uparrow \\ \uparrow \\ \uparrow \end{array} \begin{array}{c} \uparrow \\ \uparrow \\ \uparrow \end{array} \right] + \left[\begin{array}{c} \uparrow \\ \uparrow \\ \uparrow \end{array} \begin{array}{c} \uparrow \\ \uparrow \\ \uparrow \end{array} \right]$$

$$+ \sum_{\substack{\text{vectors} \neq A \\ \text{scalars} \\ \text{fermions}}} \left[\begin{array}{c} \uparrow \\ \uparrow \\ \uparrow \end{array} \begin{array}{c} \uparrow \\ \uparrow \\ \uparrow \end{array} \right] + \left[\begin{array}{c} \uparrow \\ \uparrow \\ \uparrow \end{array} \begin{array}{c} \uparrow \\ \uparrow \\ \uparrow \end{array} \right]$$

$$+ \left[\begin{array}{c} \uparrow \\ \uparrow \\ \uparrow \end{array} \begin{array}{c} \uparrow \\ \uparrow \\ \uparrow \end{array} \right] + \left[\begin{array}{c} \uparrow \\ \uparrow \\ \uparrow \end{array} \begin{array}{c} \uparrow \\ \uparrow \\ \uparrow \end{array} \right]$$

8-85
5196A22

Fig. 7

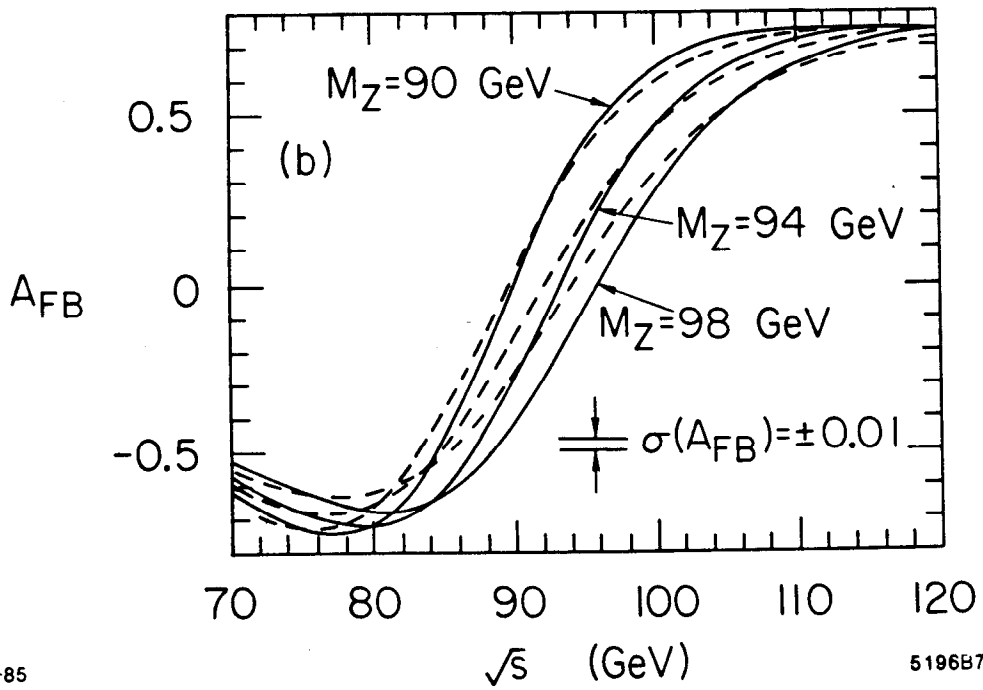
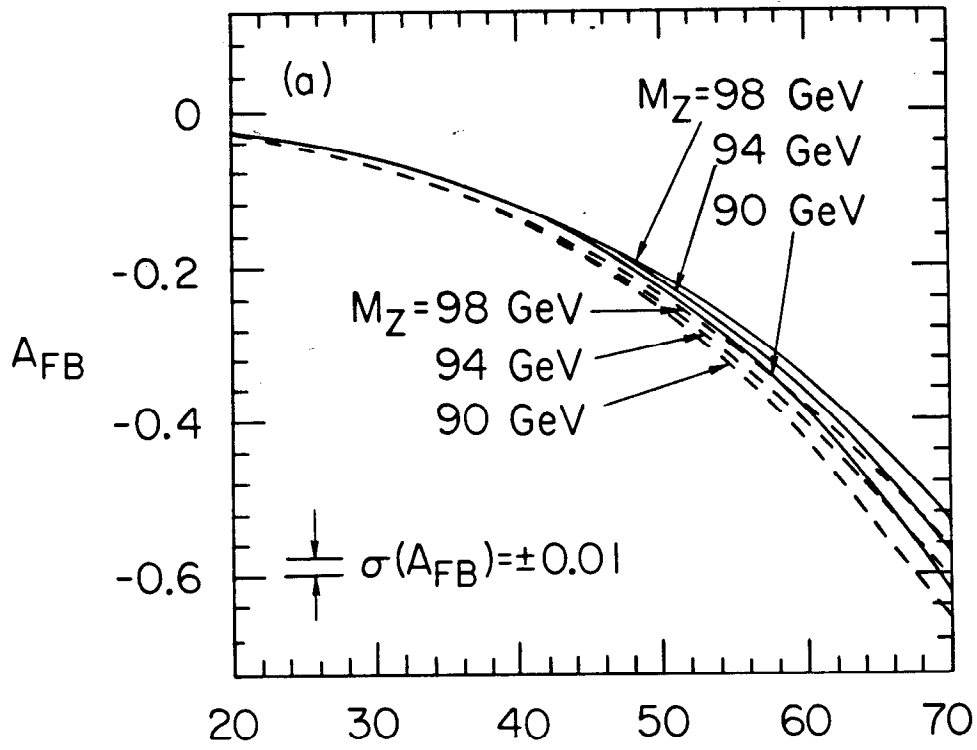


Fig. 8

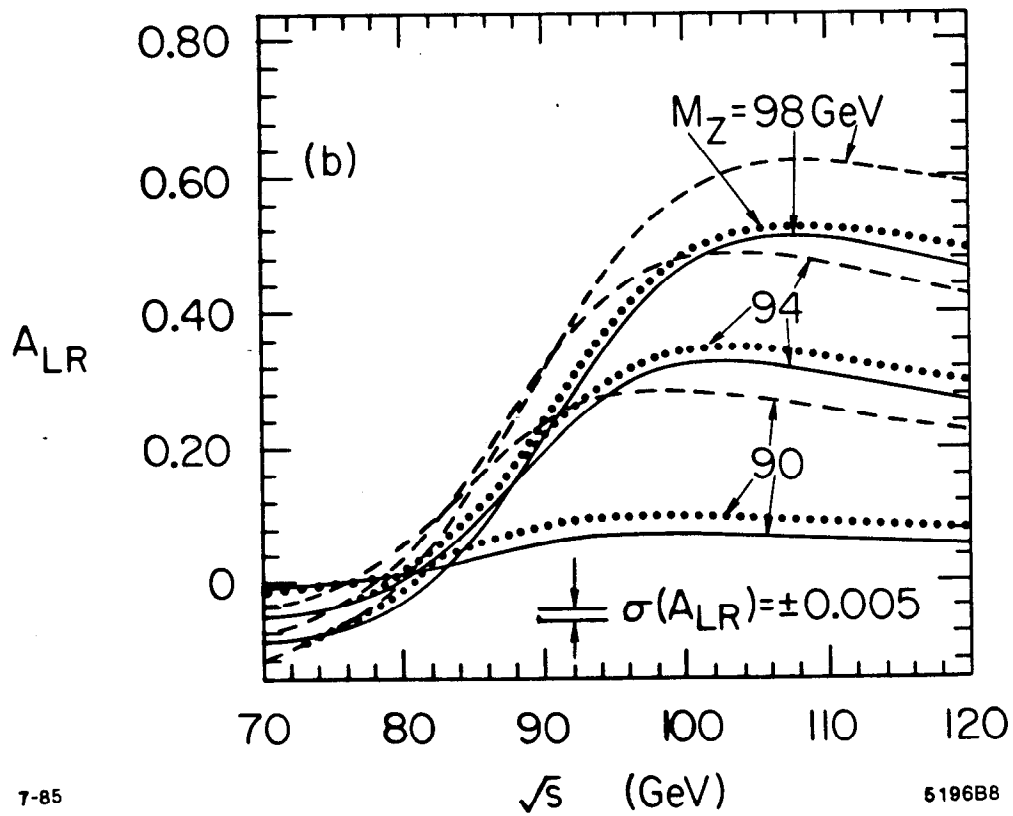
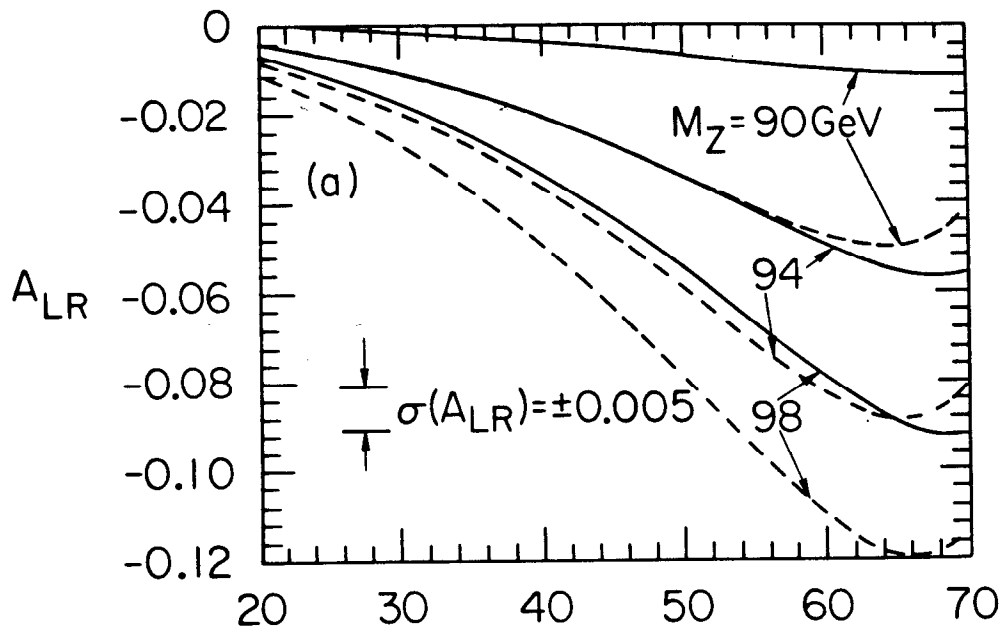
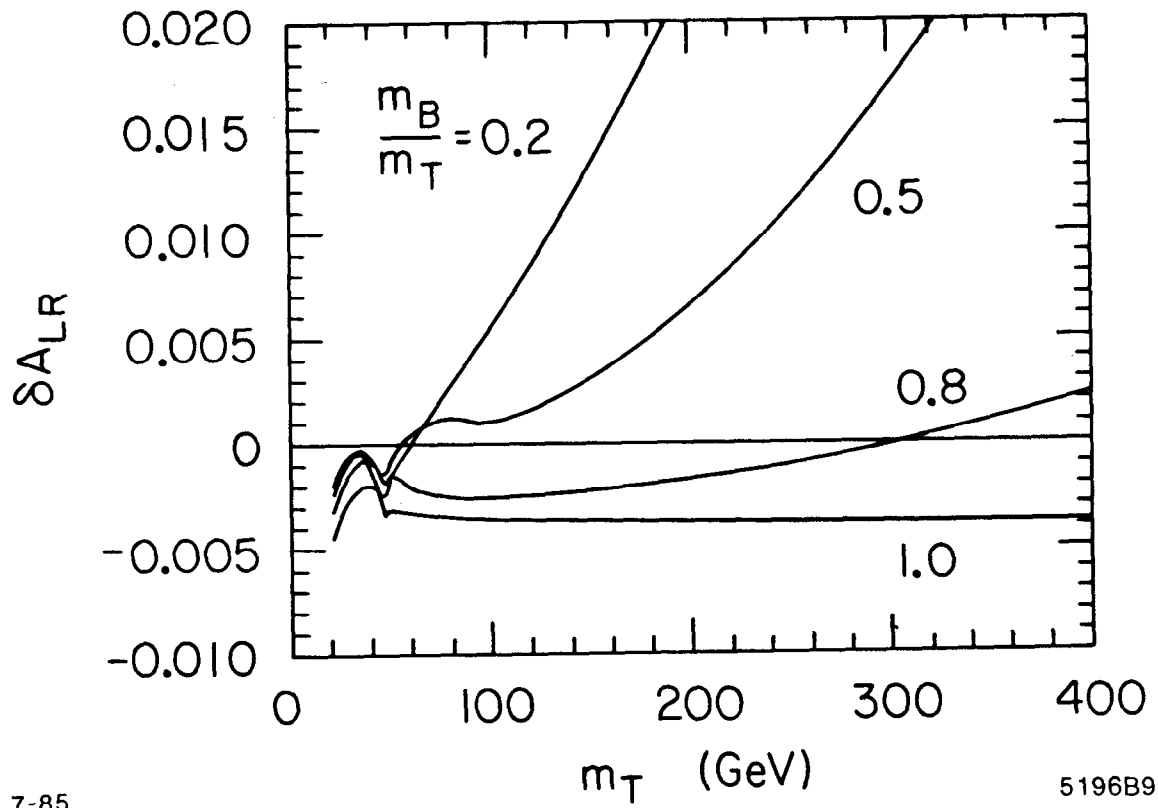


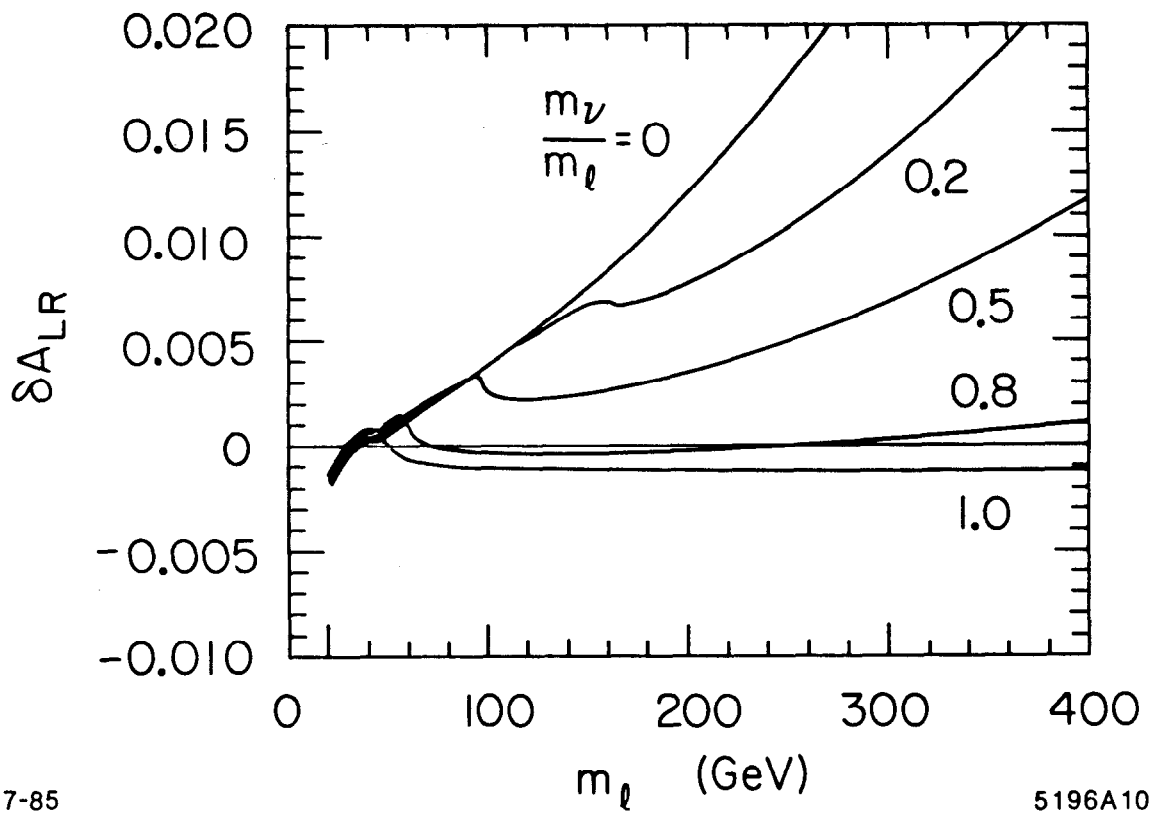
Fig. 9



7-85

5196B9

Fig. 10



7-85

5196A10

Fig. 11

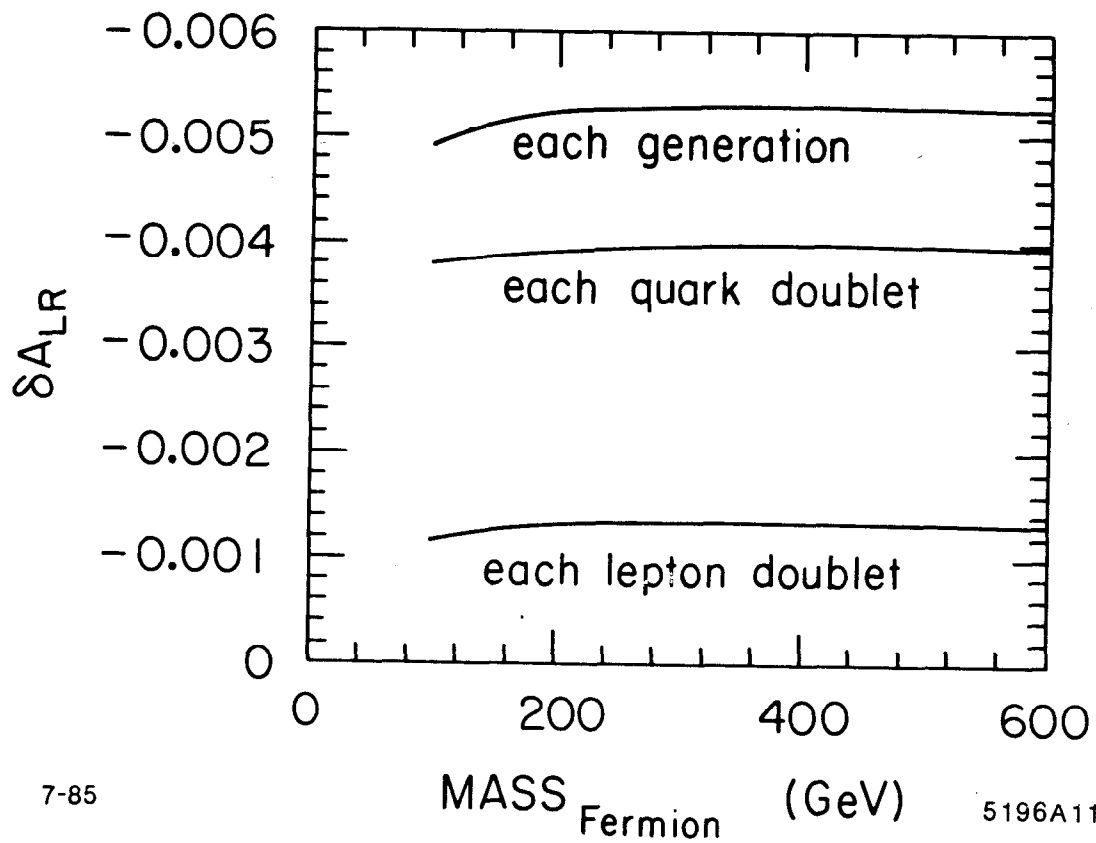
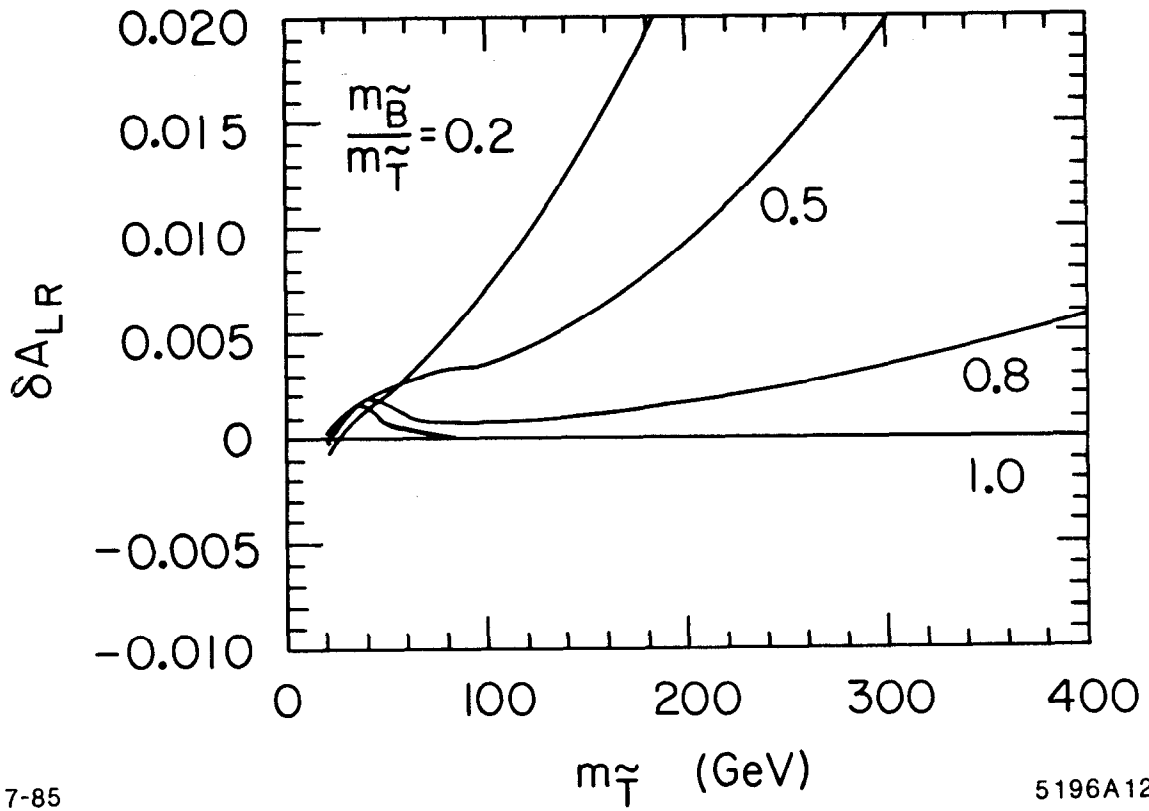


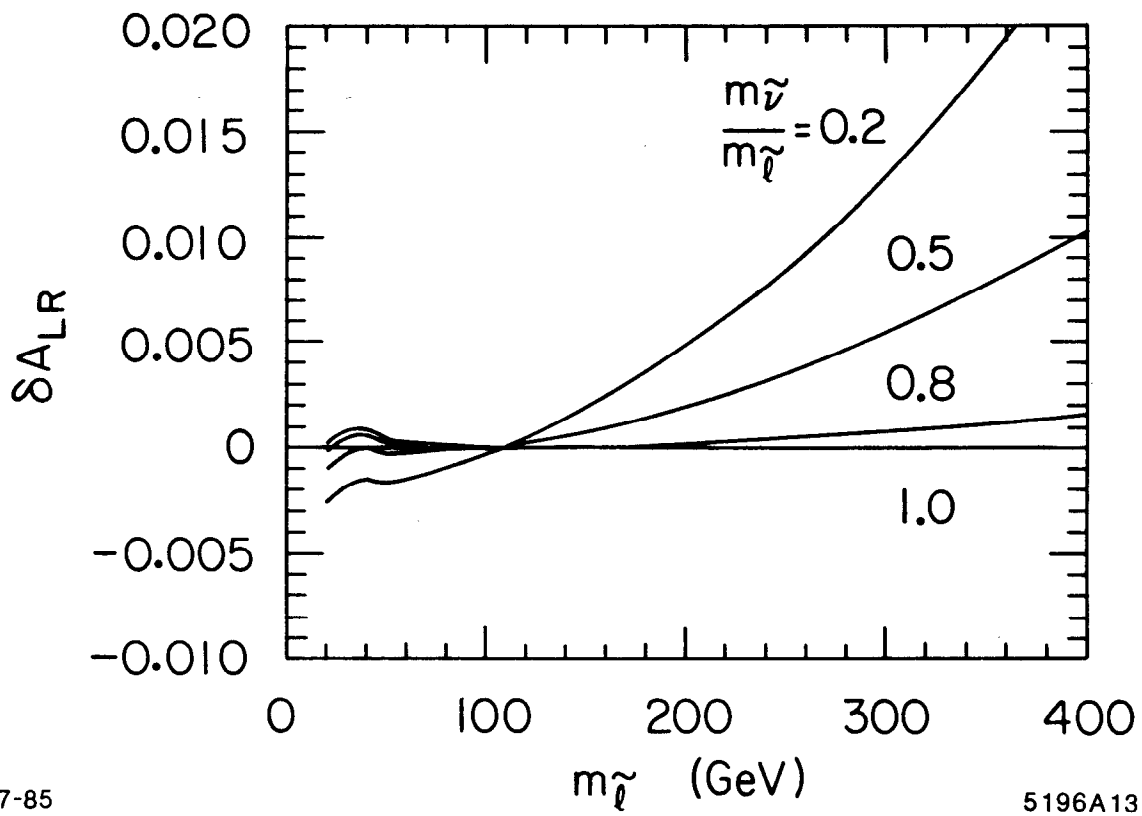
Fig. 12



7-85

5196A12

Fig. 13



7-85

5196A13

Fig. 14

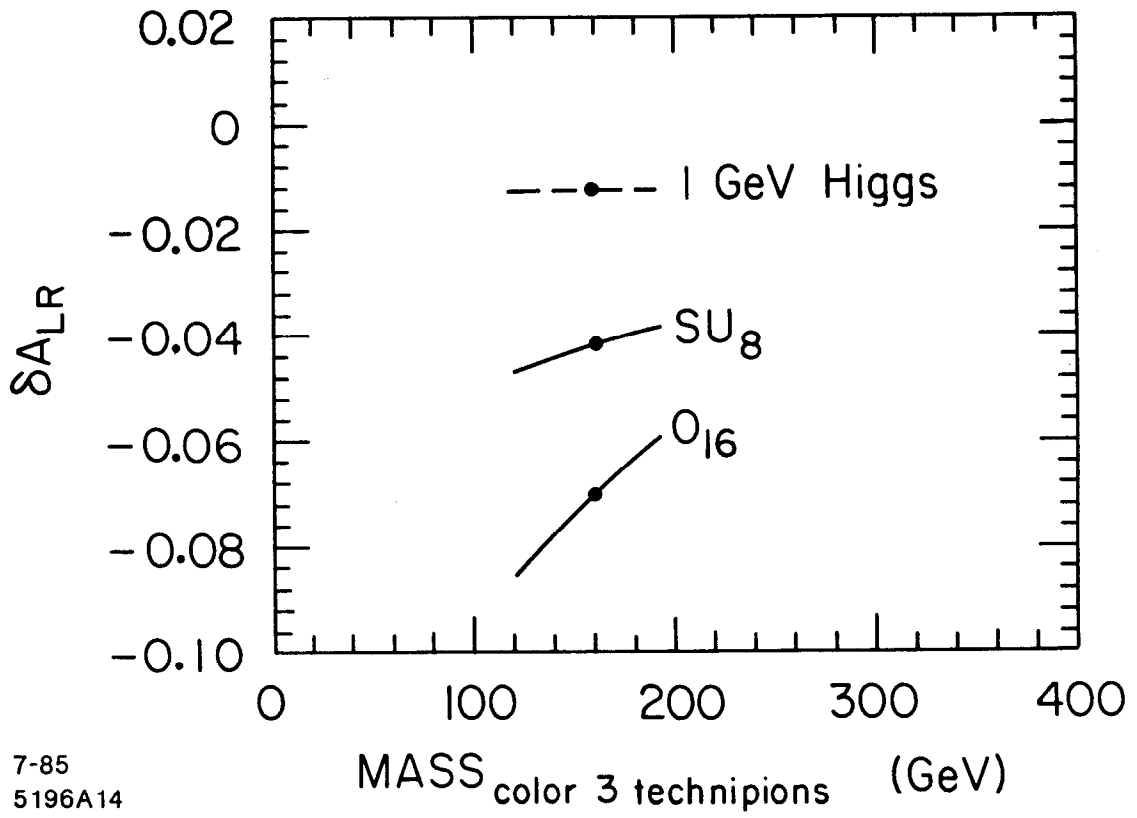


Fig 15

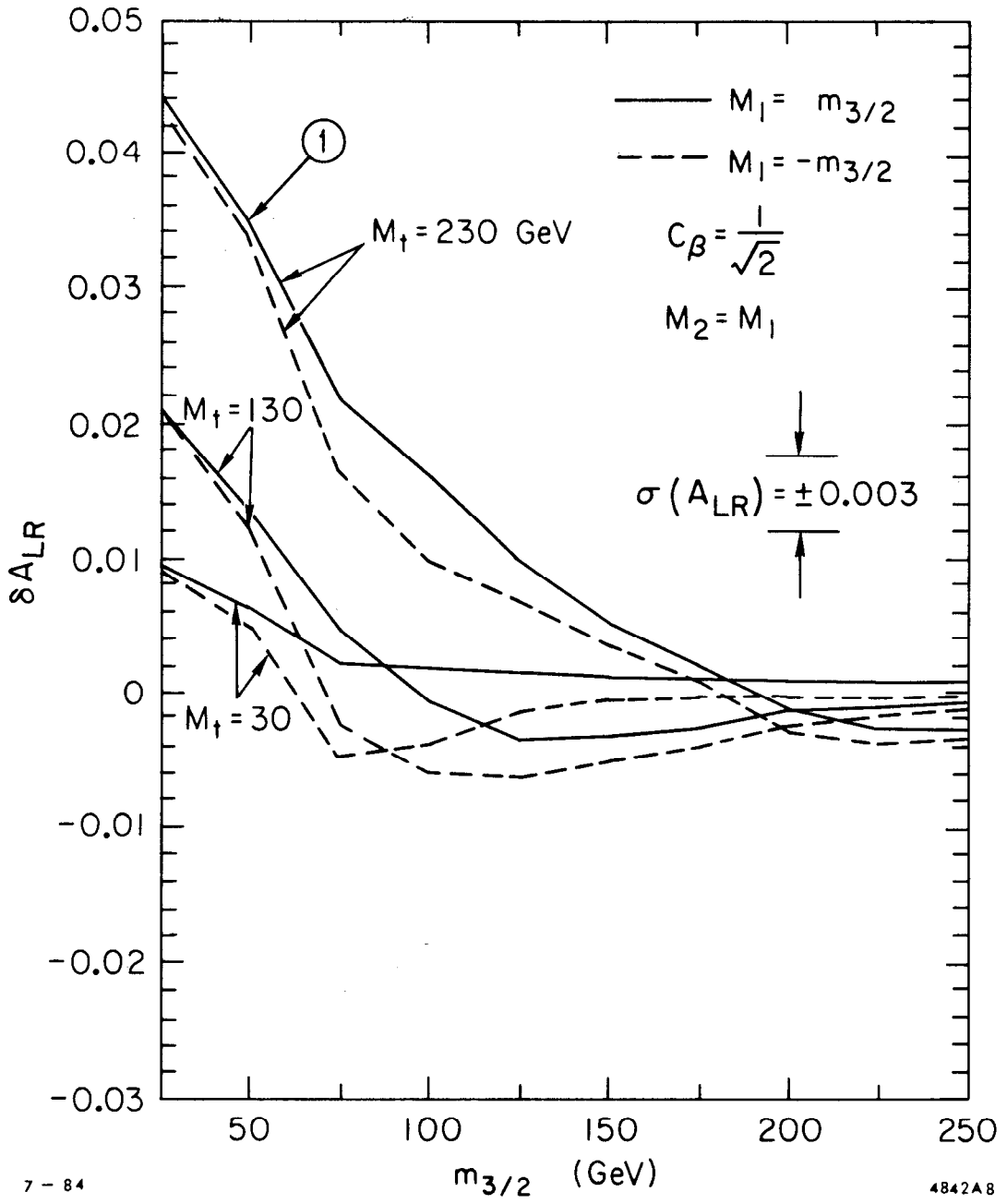


Fig. 16

Fig. 16

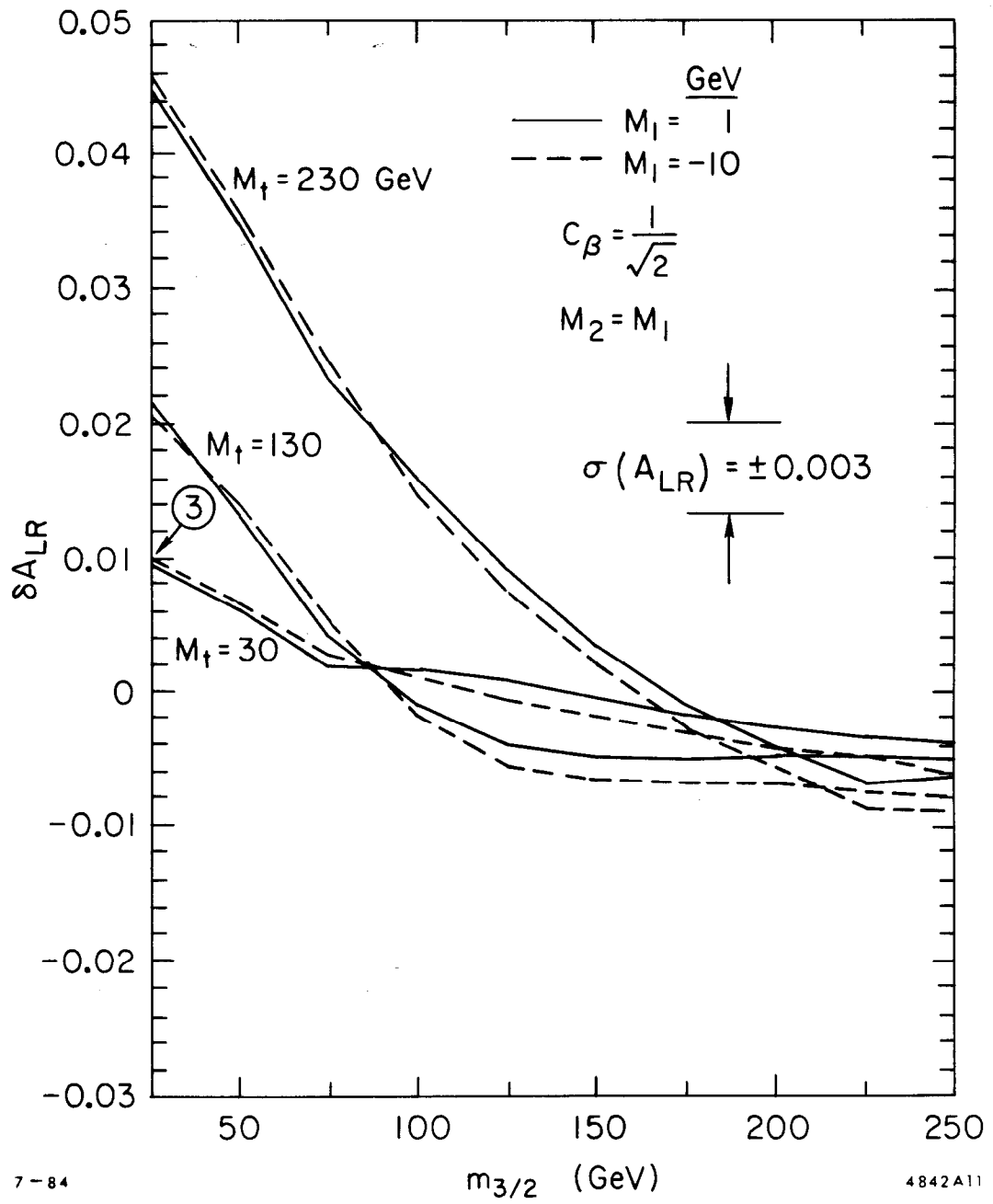
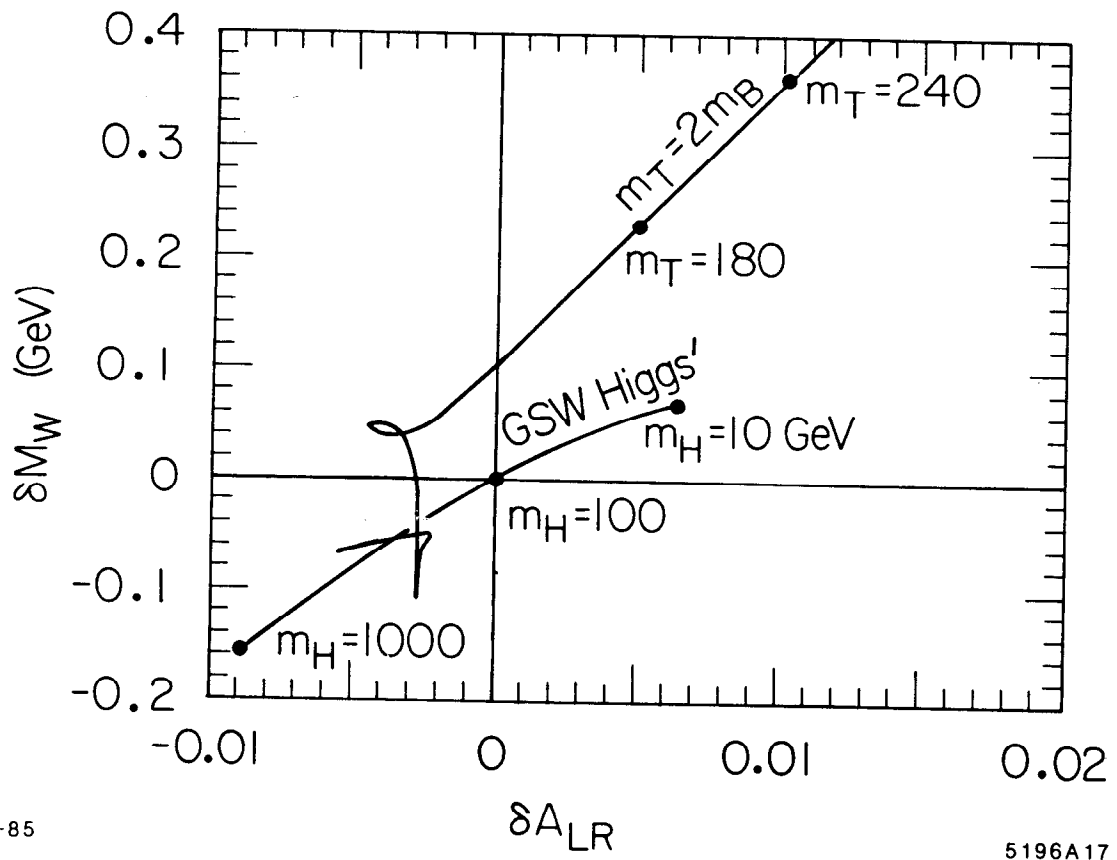


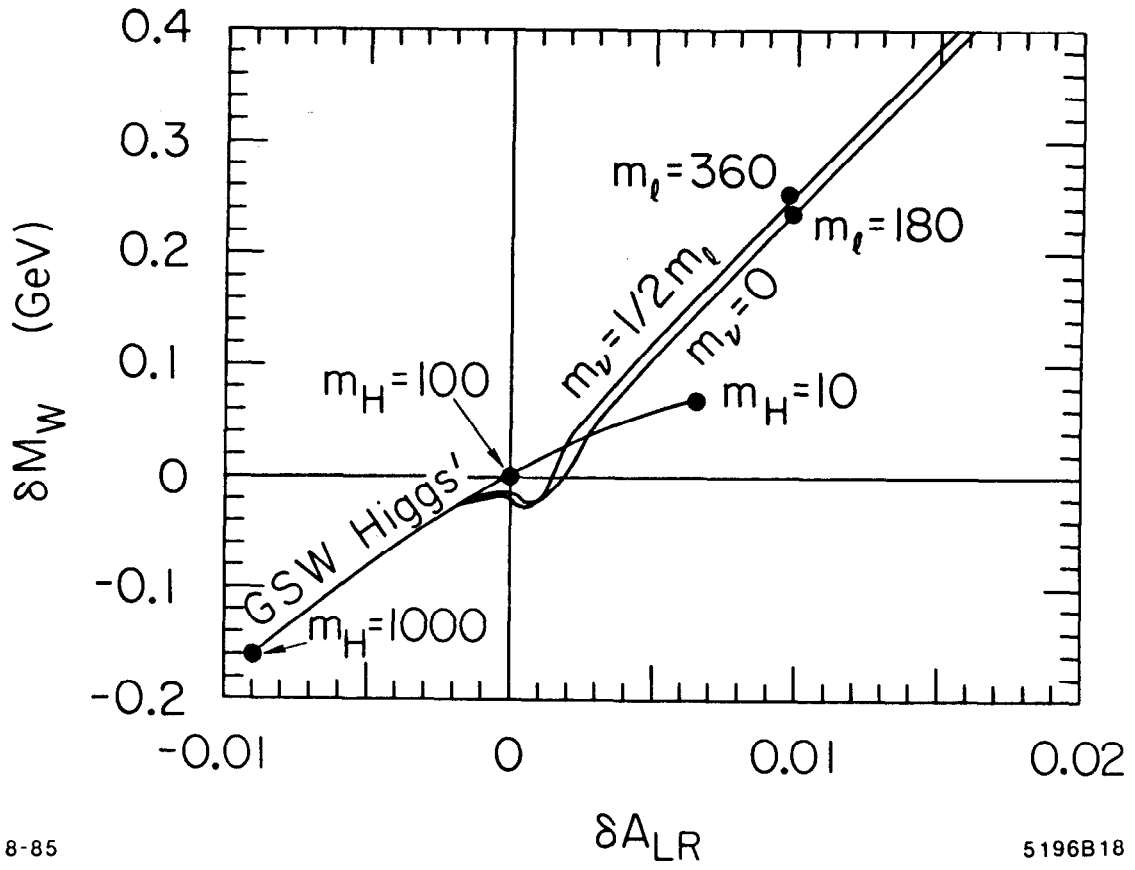
Fig. 17



8-85

5196A17

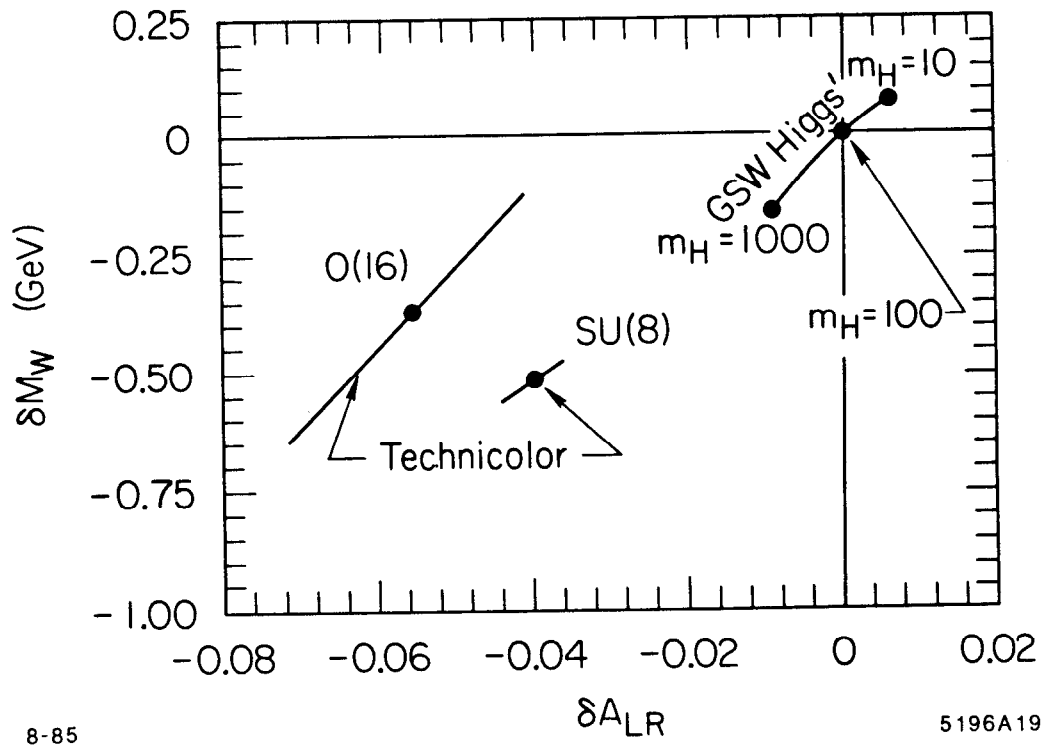
Fig. 18



8-85

5196B18

Fig. 19



8-85

5196A19

Fig. 20

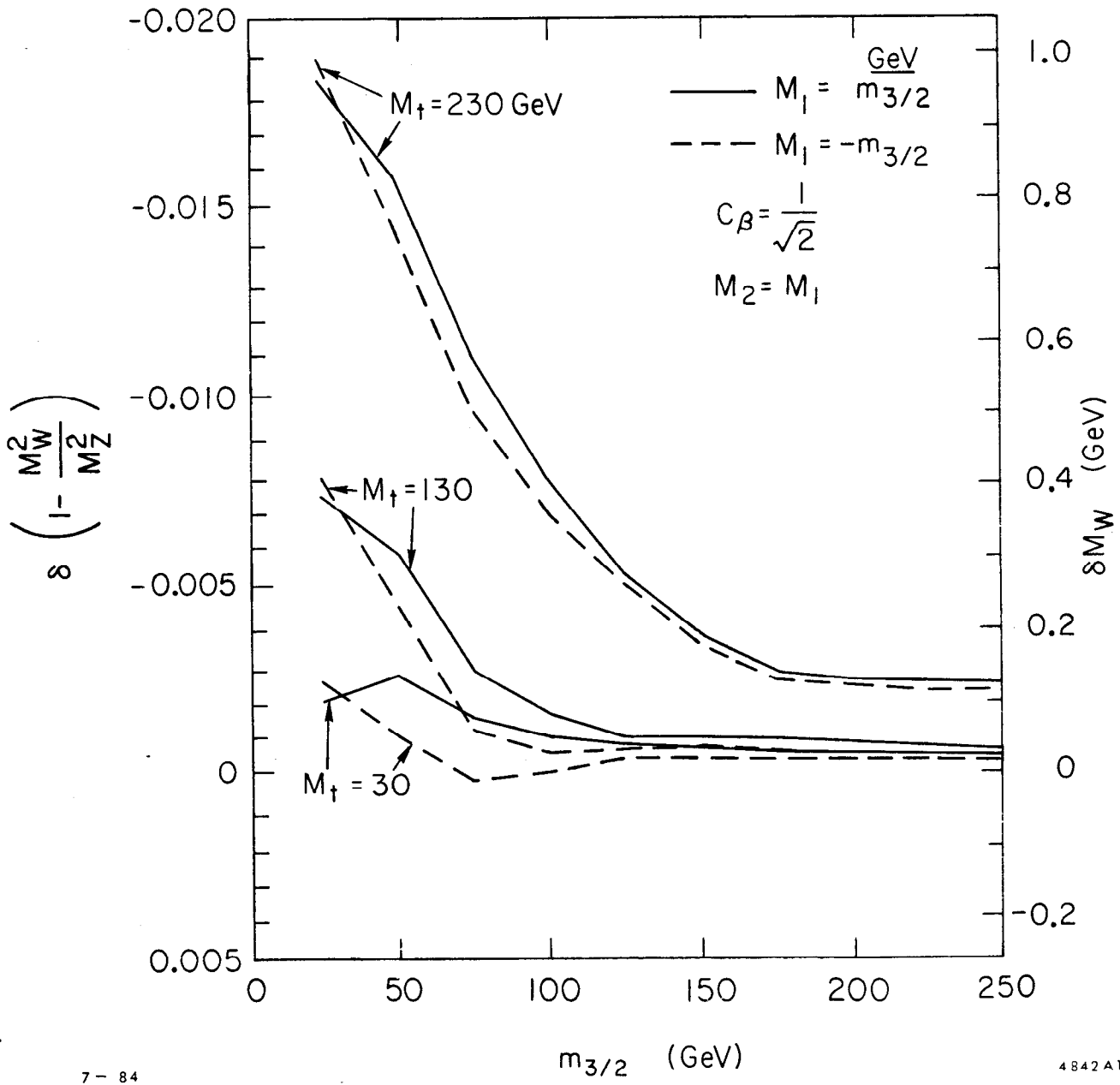


Fig. 21

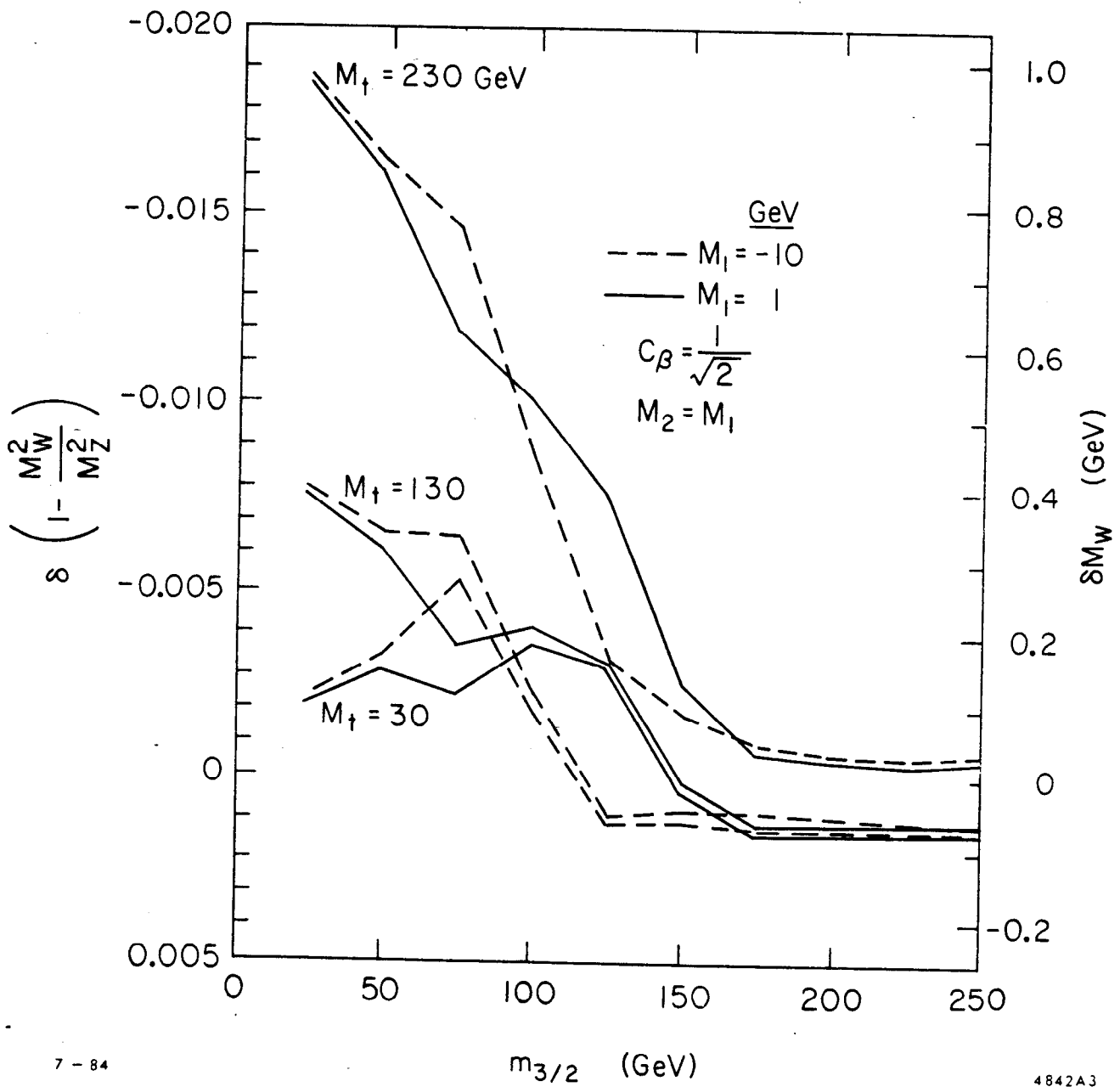


Fig. 22